

東京大学 大学院新領域創成科学研究科  
基盤科学研究系  
先端エネルギー工学専攻

平成 20 年度

修士論文

Dependency of thrust performance on thruster length and beam conditions  
for Microwave Rocket

- マイクロ波ロケット推進性能の推進器長とビーム条件依存性 -

2009 年 2 月提出  
指導教員 小紫 公也 准教授

076209 白石 裕也

# Acknowledgement

I am deeply grateful to Associate Professor Kimiya Komurasaki who gave me a challenging research theme and research environment. And his comments and suggestions were of inestimable value for my study. Moreover I also would like to appreciate the support from Professor Yoshihiro Arakawa.

Dr. Keishi Sakamoto (Plasma Heating Laboratory, Naka fusion research center, Japan Atomic Energy Agency) gave our group precious opportunities of experiments using gyrotron and some equipment at JAEA and some advice. And Mr. Atsushi Kasugai, Mr. Yukiharu Ikeda and Dr. Koji Takahashi gave us warm encouragement and some advice. On the operation of gyrotron, Dr. Ken Kajiwara, Mr. Norio Narui and Mr. Shinji Komori helped us. Especially, I am also indebt to Dr. Yasuhisa Oda whose meticulous advice and help which is not restricted to study was an enormous help to me. Whatever I say, it is not enough, but I would like to thank him. I'm so grateful to JAEA members that made it possible to complete my master thesis.

I'm obliged to Mr. Teppei Shibata, Mr. Armin Herbertz, Mr. Toshikazu Ymaguchi, and Mr. Yutaka Shimada who are Microwave Propulsion Research Group. I would like to thank all members in Arakawa-Komurasaki laboratory and department of advanced energy.

Finally, I would also like to express my gratitude to my parents and grandfather for their moral support and warm encouragements over 24 years.

# Contents

List of Figures	iii
List of Tables	vi
Nomenclature	vii
<b>Chapter 1 Introduction</b>	<b>1</b>
1.1 Back Ground of Space Engineering	1
1.2 Microwave Rocket (Beamed Energy Propulsion)	1
1.3 Thrust Generation Model of Microwave Rocket	3
1.4 Past Research of Microwave Rocket in Our Research Group	5
1.5 Objects of This Research	6
<b>Chapter 2 Experimental Apparatus</b>	<b>7</b>
2.1 Japan Atomic Energy Agency	7
2.2 Gyrotron	8
2.3 Thruster Model	10
2.4 Thrust Measurement	10
2.4.1 Pressure Gauge	10
2.4.2 Load Cell	13
2.5 Air-Breathing System	18
2.6 Chamber	20
2.7 High Speed Camera	21
<b>Chapter 3 Single Pulse Condition</b>	<b>22</b>
3.1 Pulse Width and Thruster Length	22
3.2 Pressure in the Thruster	25
3.3 Microwave Power	26
3.4 Dependency on Pressure and Microwave Power	27

3.5	Thrust Performance by Gaseous Species	30
3.6	Conclusion of Single Pulse Condition	34
<b>Chapter 4</b>	<b>Multi-Pulse Condition</b>	<b>35</b>
4.1	Thrust Recovery by Partial Filling Rate	35
4.2	Impulse Dependence on $u_0$ and $f$	35
4.3	Dependence on the Partial Filling Rate	37
4.4	Contribution of Plasma Length in Low Partial Filling Rate Region	38
4.5	Self Air-Breathing	40
4.6	Conclusion of Multi-Pulse conditions	42
<b>Chapter 5</b>	<b>Thrust Optimization</b>	<b>43</b>
5.1	Thrust Optimization in single pulse condition	43
5.2	Thrust Optimization in multi-pulse condition	45
5.3	Thrust Optimization	46
5.4	Flight Mode	47
5.5	Flight Analysis	49
<b>Chapter 6</b>	<b>Conclusion</b>	<b>57</b>
<b>References</b>		<b>59</b>
<b>Appendix</b>		<b>61</b>
	• Graph of photograph ionization front propagation by High speed of plasma (x axis: Pressure, y axis: microwave power density)	62

# List of figures

1.1	The schematic figure of Microwave Rocket	3
1.2	Schematics of the pressure distribution evolution along the longitudinal direction	4
1.3	Dependence of $U_{\text{shock}}$ and $U_{\text{ioniz}}$ on $S_0$	6
2.1	Maps of JAEA Naka	7
2.2	Gyrotron	8
2.3	History of microwave pulse	9
2.4	History of microwave pulse	9
2.5	Amplifier	11
2.6	Pressure Element	11
2.7	Thruster model with pressure gauge	12
2.8	Thruster model with pressure gauge	12
2.9	Pressure history at thrust wall by pressure element	12
2.10	Load Cell	13
2.11	Thruster model with load cell	13
2.12	Calibration Result for thrust impulse	15
2.13	Calibration Result for steady thrust	16
2.14	Load Cell Output ( $P=200\text{kW}$ , $f=50\text{Hz}$ )	16
2.15	RF Signal ( $P=200\text{kW}$ , $f=50\text{Hz}$ )	17
2.16	Comparison of thrust measurement of pressure element and load cell	17
2.17	Electric valves for flow operation	18
2.18	Thruster model with forced air-breathing system	19
2.19	Thruster model with all equipment for experiment	19
2.20	Thruster model with all equipment for experiment	20
2.21	Chamber	21
2.22	High Speed Camera	21
3.1	Thrust impulse dependence on pulse width; $L=590\text{mm}$	23
3.2	Momentum coupling coefficient dependence on pulse width;	

	L=590mm	23
3.3	Momentum coupling coefficient dependence on normalized plasma length; L=590mm	24
3.4	Momentum coupling coefficient dependence on pulse width at each ambient pressure; L=300mm	24
3.5	Thrust Impulse dependence on pressure in the thruster; L=100, 300mm	25
3.6	The high speed camera photograph of plasma ( Atmosphere pressure:1.0atm, 0.5atm, 0.1atm )	25
3.7	Momentum Coupling Coefficient dependence on pressure in the thruster; L=300mm	26
3.8	Momentum coupling coefficient dependence on pressure in the thruster and microwave power density	27
3.9	Ionization front propagation velocity and shock wave propagation velocity dependence on pressure in the thruster (Plasma: ionization front propagation velocity, shockwave: shock wave propagation velocity)	29
3.10	Maximum value of momentum coupling coefficient dependence on pressure in the thruster and microwave power density ( prediction)	30
3.11	rust Impulse dependence on Pulse width at each ambient pressure ( $\phi 60$ parabola reflector+ Rectangle tube(L=320mm))	31
3.12	Momentum coupling coefficient dependence on pulse width at each ambient pressure	32
3.13	Thrust Impulse dependence on Pulse width at each ambient pressure ( parabola reflector )	34
4.1	Thrust impulse for each pulse count in repetitive pulse operations $f=50\text{Hz}$ and $L=390\text{mm}$	36
4.2	Steady impulse for various $u_0$ and pulse repetition frequencies $P=300\text{kW}$ , $L=390\text{mm}$	36
4.3	Thrust impulse dependence on the partial filling rate; Symbols show measurements and a solid line does theoretical prediction. Steady impulse for various $u_0$ and pulse repetition frequencies	37

4.4	Normalized thrust dependence on partial filling rate	39
4.5	Normalized thrust dependence on partial filling rate (evaluated by $l$ )	39
4.6	2nd thrust impulse with no forced air-breathing	30
4.7	Pressure history at thrust wall by pressure element	41
5.1	Flight Mode of Microwave Rocket	49
5.2	Flying speed in flight analysis (vertical launch, microwave power: 1.2 [GW])	50
5.3	Flying altitude in flight analysis (vertical launch, microwave power: 1.2 [GW])	51
5.4	Flying speed in flight analysis (parallel flight, microwave power: 1.2 [GW])	52
5.5	Flying altitude in flight analysis (parallel flight, microwave power: 1.2 [GW])	52
5.6	Flying speed in flight analysis (vertical launch, thrust is constant)	53
5.7	Flying altitude in flight analysis thrust is constant	54
5.8	Normalized microwave power	54
5.9	Integrated normalized microwave power	55
5.10	Flying speed dependence on integrated normalized microwave power	55

## List of tables

3.1	Gaseous ionization voltage	32
4.1	Experimental Conditions	39
5.1	The feature in each flight mode	47



## Nomenclature

$\tau$	: Pulse Width of Microwave
$A$	: Area of the thrust wall
$a$	: Sonic speed at the region
$C_m$	: Momentum coupling coefficient
$d$	: Dismeter of the thruster model
$F$	: Thrust force
$f$	: Microwave repetitive frequency
$I$	: Thrust impulse
$I_{single}$	: Thrust impulse at first pulse of microwave
$L$	: Thrust length
$L_{thruster}$	: Thrust length
$L_{plasma}$	: Ionization traveling length
$l$	: Normalized plasma length
$P$	: Microwave Power
$p$	: Pressure in the thruster model
$p_n$	: Pressure in the thruster model at the region
$S_0$	: Microwave Power Density
$t$	: Time
$T_{plateau}$	: Duration time of constant pressure at the thrust wall
$u$	: Forced flow velocity in the thruster model
$U_{ioniz}$	: Propagation velocity of ionization front
$U_{shock}$	: Propagation velocity of shock wave

$V$  : Replaced Air Volume

$x$  : Streamwise coordinate

$u/Lf$  : Partial Filling Rate

# Chapter 1

## Introduction

### 1.1 Background of space development

Now, the space development must be needed for not only the intellectual curiosity use's but also military use's and our life. For example, a meteorological satellite, GPS, a communications satellite and microgravity use and so on. And recently, the limelight is exposed to the space trip. But huge cost is needed for not only satellite but also the rocket which conveys to the universe a satellite for these space development. The launch cost is about 1 million yen per 1kg payload. This cost is an barrier of space development expansion.

The only way of space transportation is a chemistry rocket under the status quo, though there is electric propulsion and so on in space propulsion. Chemical rocket is a rocket which carries fuel and oxidizer, makes the gas of high temperature and high pressure inject by the chemical reaction of fuel and oxidizer, and obtains thrust according to the reaction. As the combination, the combination of "hydrazine and nitrogen tetroxide", " kerosene and liquid oxygen" and " liquid hydrogen and liquid oxygen" has been used. Moreover, research of hybrid rockets using acrylics and liquid oxygen is also done. But rockets of this type need complex components such as a burner and turbo pumps and are wasted after used once. Furthermore, the payload ratio is several percent since fuel forms about 90% of rocket weight. This is a reason which takes huge cost for a launch.

As mentioned above, the structure of a rocket is simple, a payload ratio is high, and dramatically cheap propulsion system is expected.

### 1.2 Microwave Rocket (Beamed energy propulsion)

There is beamed energy propulsion as a propulsion system which solves the problem of chemistry rocket. The schematic figure of a microwave rocket is shown in Figure 1.1.

In beamed energy propulsion, a thruster is supplied beamed energy from

outside of the thruster such as ground based beam sources and converts the energy to thrust. In air breathing mode, there is no necessity of carrying fuel since air can be used as fuel. Furthermore, equipment such as a combustor and a turbine pump is unnecessary and structure is simple. Although huge cost is needed for the source of an oscillation of a beam, the cost is refunded with the increment in the count of a launch since rocket structure is simple. [1] As mentioned above, high payload ratio and dramatically cheap launch cost are expected.

In beamed energy propulsion, research, a method to use a laser or microwave as an energy source has been main stream.[2] Kantrowitz suggested beamed energy propulsion using the laser beam from facilities on the ground or in the space in 1972. [3] Raizer et al figured out a laser energy conversion process as Laser Supported Combustion and Laser Supported Detonation around the same time. [4] In 1998, Myrabo et al. demonstrated flight test with Lightcraft and a CO<sub>2</sub> pulse laser. [5, 6]

The laser can travel with low diffusion. Beamed energy propulsion requiring long distance transmission needs features of the laser. But beamed energy propulsion asks large output of an energy source. Current laser sources can't make an output to be able to apply beamed energy propulsion. On the other hand, microwave generator which is gyrotron are being developed as heat source of nuclear fusion in Japan Atomic Energy Agency and a microwave has already realized 1MW beam sources. Furthermore, 1GW class output is expected by phased array technology. Thus a microwave source which has an output to be able to apply beamed energy propulsion will be realized in not so distant future.

In our research group, Microwave Rocket [10-18] is developed using 1MW gyrotron. [7-9]

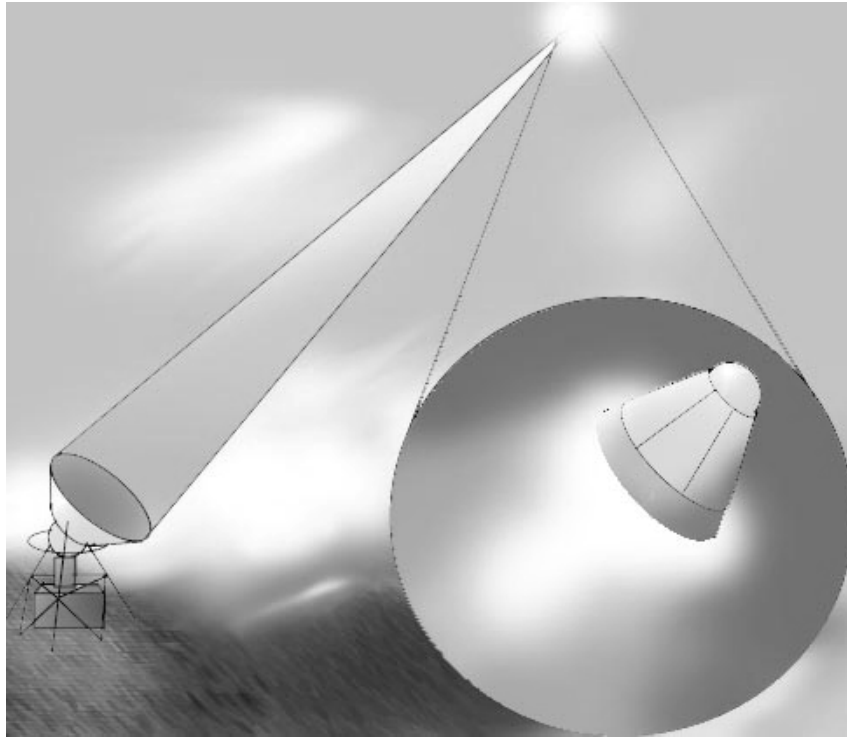


**FIGURE 1.1.** The schematic figure of Microwave Rocket

### **1.3 Thrust generation model of Microwave Rocket**

Thrust generation model of Microwave Rocket is explained. Figure 1.2 shows the Microwave Rocket engine cycle. It has been proposed based on a pulse detonation engine model.

A cylindrical body has a closed end and an open end. The closed end is called a thrust wall. In pulse detonation engine, combustion in a thruster drives a shock wave and pressure at the thrust wall is maintained higher than ambient/initial pressure during the period from the ignition at the thrust wall to the arrival of an expansion wave coming back from the open end. [19, 20] In the Microwave Rocket model, the combustion is replaced by microwave heating. When microwave is inputted towards the reflector in the thrust wall, plasma generate near a thrust wall. This plasma absorbs the microwave which comes later and drives a shock wave. The shock wave propagates to a thruster outlet with the ionization front in the thruster. When a shock wave passes a thruster outlet, an expansion wave propagates towards a thrust wall from a thruster outlet, and an exhaust gas will be made. The high pressure is maintained until this

expansion wave reaches a thrust wall in near a thrust wall. An impulse gained during a cycle is equal to a product of the pressure kept at the thrust wall and the period from the ignition to the arrival of the expansion wave. This cycle is repeated and Microwave Rocket generates thrust intermittently.

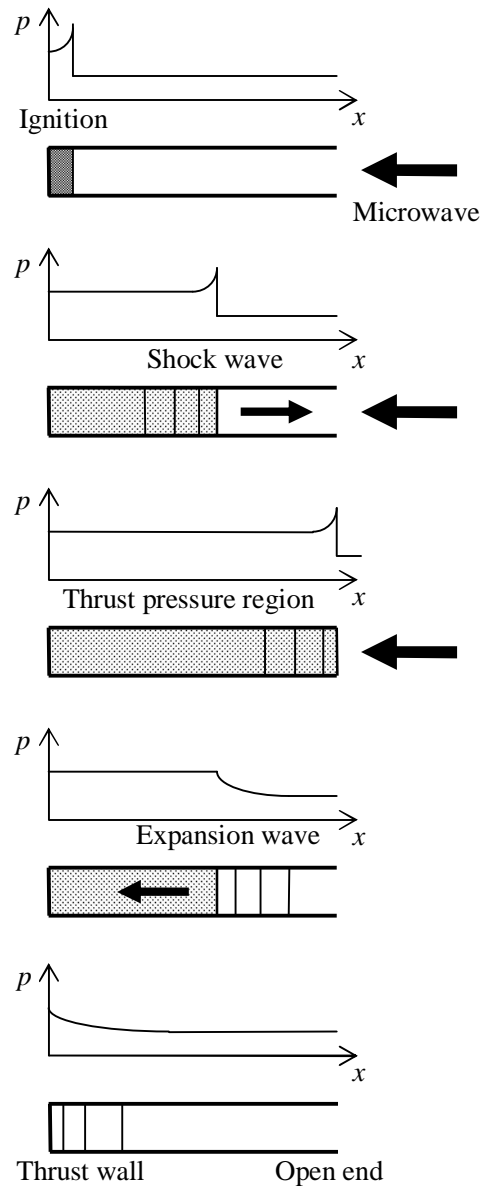


**FIGURE 1.2.** Schematics of the pressure distribution evolution along the longitudinal direction

## 1.4 Past research of Microwave Rocket in our research group

Flight experiments were conducted with a single microwave pulse. Flight passes of the thruster along to altitude direction were measured by a laser displacement gauge. Impulses were calculated from initial velocity of the thruster. We estimated performance of Microwave rocket using impulses  $I$  and momentum coupling coefficients  $C_m$  defined as a ratio of impulses to input energy of the microwave was estimated. In these experiments  $I$  and  $C_m$  dependences on microwave power, thruster length and width of a microwave pulse were figured out. Flight experiments with multi microwave pulses were conducted too. Impulses gaining from 2nd pulse decrease to 50-60% of Impulses gaining from 1st pulse. The cause that impulses decrease was thought to be changing conditions inside of the thruster by 1st pulse. It was suggested to exhaust the high temperature gas remaining in the thruster by front air breathing.

To install air breathing system and to observe inside of the thruster, thrust measurement using fixed thruster was required. Two pressure gauges were mounted near the thrust wall and the open end of the fixed thruster. Impulses were estimated from pressure history at the thrust wall with pulse detonation engine model and well agreed with results of flight experiments. Thrust estimation of the fixed thruster was enabled.

Synflex tubes connect high pressure tank and the thrust wall side of the thruster. High pressure generates a flow in the thruster as an air breathing thruster. The flow exhausts high temperature gas and improves impulses obtained by microwave pulses since the second. Therefore 1sec endurance operations were conducted successfully.

Thrust measurements by pressure history make observation in the thruster possible too. Propagation velocities of the shockwave  $U_{\text{shock}}$  and the expansion wave  $a_3$  were measured from differences between arrival times of each wave. A high speed camera captured propagation velocities of the ionization front  $U_{\text{ioniz}}$ .  $U_{\text{shock}}$  and  $U_{\text{ioniz}}$  increase with the peak microwave power density  $S_0$  as shown in Figure 1.3. [15]

In the high  $S_0$  region,  $U_{\text{shock}}$  and  $U_{\text{ioniz}}$  is almost same. The region is called Overdriven Microwave Supported Detonation (Overdriven MSD). In the low  $S_0$  region  $U_{\text{shock}}$  was larger than  $U_{\text{ioniz}}$  and the shock wave and the ionization front had separated. The region is called Microwave Supported Combustion (MSC). The middle region is

called C-J Microwave Supported Detonation (C-J MSD).

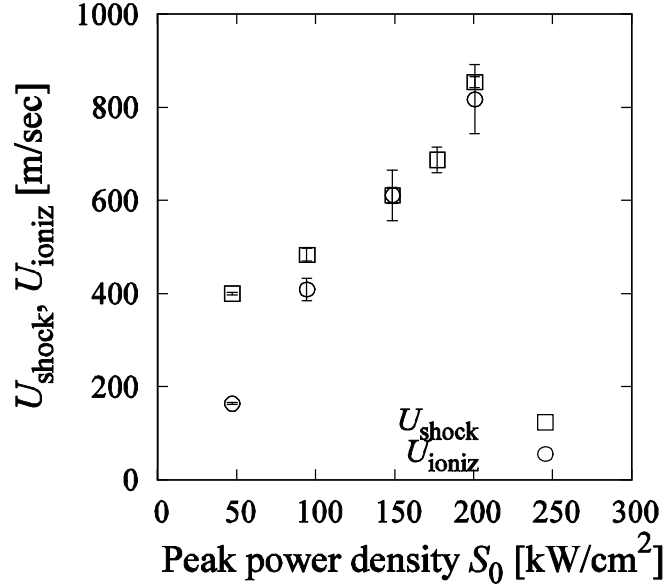


**FIGURE 1.3.** Dependence of  $U_{shock}$  and  $U_{ioniz}$  on  $S_0$  [15]

## 1.5 Objects of this research

The purpose of this research is to optimize the thrust which is considered to be the most important for microwave rocket realization. There are a microwave condition, a thruster condition, atmosphere conditions and so on as a component which determines the thrust of a microwave rocket. Therefore, optimized thrust condition is verified by changing pulse width, thruster length, pressure in the thruster and gas species on the single pulse conditions of microwave. Furthermore, an air breathing system is established for against the thrust reduction after 2nd pulse on microwave repetitive conditions of microwave, and thrust recovery and thrust dependence on partial filling rate was verified.

Thrust optimization of a microwave rocket is done by verifying required conditions for the demanded thrust performance in the time of an actual flight using these results.



## Chapter 2

### Experimental Apparatus

#### 2.1 Japan Atomic Energy Agency

In Japanese Atomic Energy Agency, the research and technical development about atomic power (nuclear fission, nuclear fusion) are done. Japanese Atomic Energy Agency, unified Japan Atomic Energy Research Institute and Japan Nuclear Cycle Development Institute, was inaugurated in October, 2005. This research was joint research of the University of Tokyo and Japanese Atomic Energy Agency using RF test stand (RFTS). Thus, the experiment was conducted by the Japanese Atomic Energy Agency Naka nuclear fusion research institute heating engineering research group in Naka city, Ibaragi Prefecture.

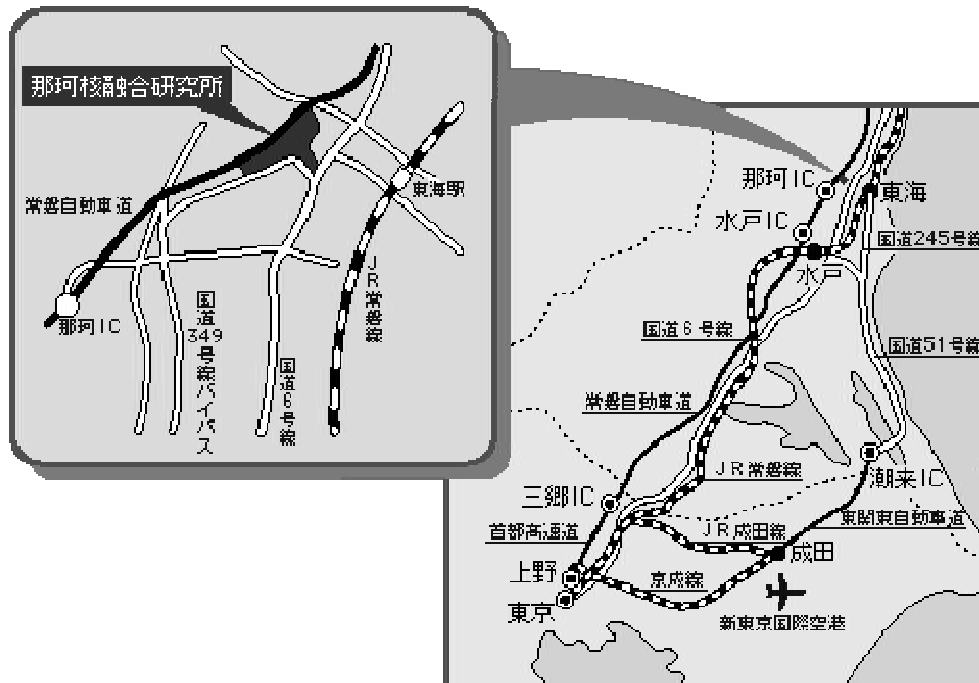
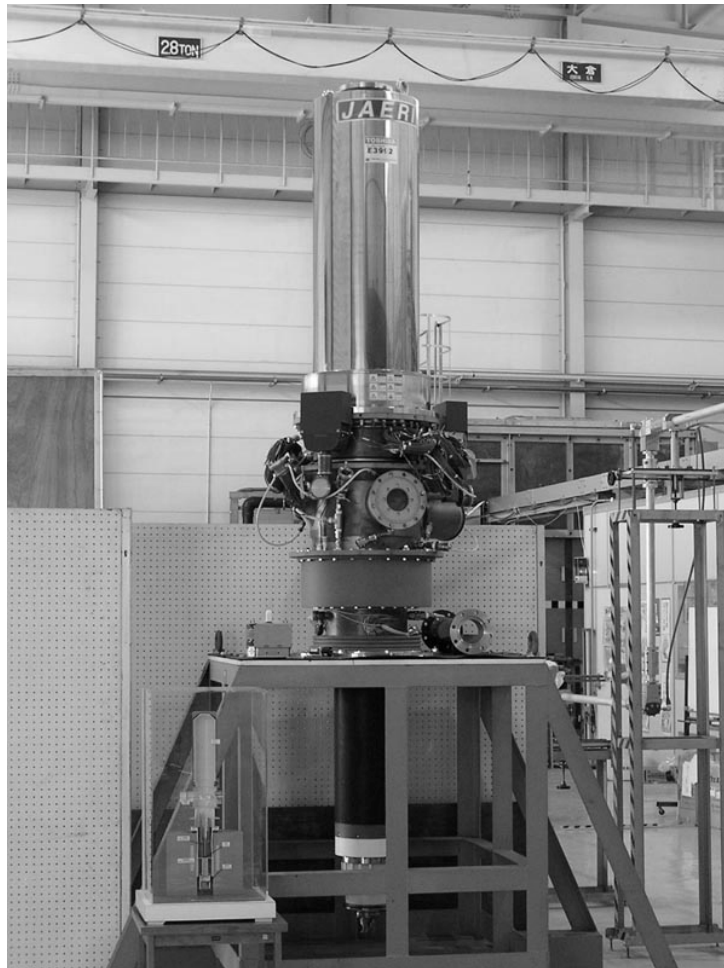


FIGURE 2.1. Maps of JAEA Naka

## 2.2 Gyrotron

A 1MW-class 170GHz gyrotron which is shown in Figure 2.2 was used as a microwave generator. [21] A gyrotron is the millimeter wave and submillimeter wave light source whose oscillation principle is the electron cyclotron resonance Mazur action using mass change of the electron by the relativity effect.



**FIGURE 2.2.** Gyrotron

A gyrotron consists of a magnetron incidence type electron gun which produces a rotation electron beam, a hollow resonator which interacts with an electron beam and oscillates RF, a mode converter which changes the produced wave guide tube mode RF into an electromagnetic wave beam, a collector which absorbs the electron beam which finished the interaction, and an output window which stops a vacuum and outputs RF.

The gyrotron was developed for high frequency induction heating of an International Thermonuclear Experimental Reactor (ITER) in Japanese Atomic Energy Agency. 1MW operation from 0.1msec to 1000sec is possible about the microwave power. Moreover, 3600sec about microwave duration is attained in the case of 800kW operation. This is almost twice time which ITER needs. The microwave beam is Gaussian and its beam waist is 20.4mm. [8] History of microwave pulse is shown in Figure 2.3 and 2.4.

In this study, controlling oscillation mode realized repetitively pulsed operation by modulation to the accelerating voltage of an electron beam. At single pulse operation, the duration and power of each pulse was fixed at about 20 $\mu$ sec-2.0msec and 190-840kW, respectively. At repetitively pulse operation, the duration and power of each pulse was fixed at about 1.3-2.6msec and 200-270kW, respectively. The repetition frequency was varied from 5Hz to 50Hz and the maximum operation time is 1sec.

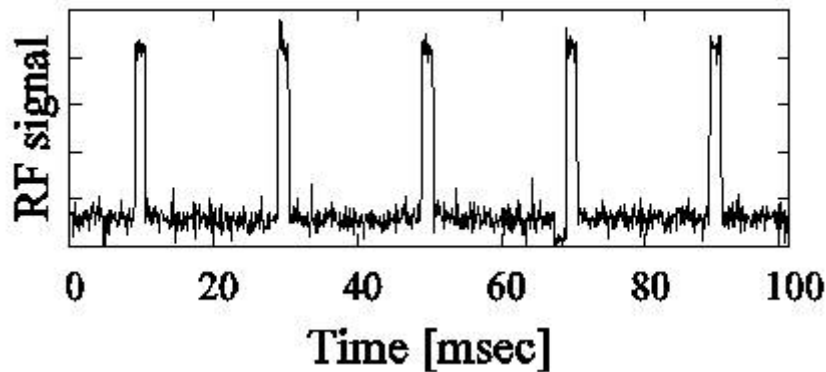


**FIGURE 2.3.** History of microwave pulse

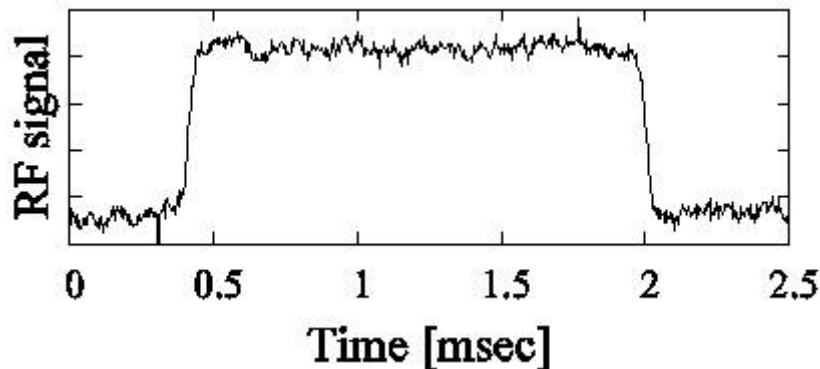


**FIGURE 2.4.** History of microwave pulse

## **2.3 Thruster Model**

A cone-cylinder shape thruster model was used as shown in Figures 2.3 and 2.4. It consists of an acrylics cylinder and an aluminum conical reflector which functions as a thrust wall. The thruster length was varied from 0.19m to 0.69m and diameter is fixed at 60mm.

## **2.4 Thrust Measurement**

In this research, thrust measurement of the microwave rocket was done using the thrust stand which used the pressure element and the load cell. The generated impulse of each pulse was measured by the pressure element, and the average thrust was measured by the load cell. In the past research, thrust measurement by a pressure element was done. However, thrust analysis time has increased as microwave repetitive frequency increases. The analysis time of an average thrust can be dramatically shortened by the thrust stand using a load cell. On the other hand, although the load cell can measure an actual thrust value direct, it supplemented with the data based on a pressure history, since the error of a tube or a cable can be considered. Moreover, since the thrust stand using a load cell cannot be set in a chamber, calculation by a pressure element is needed. Thereby, the optimal thrust measuring method can be chosen according to experiment conditions.

In this section, thrust measurement of a pressure element and a load cell is explained.

### **2.4.1 Pressure Element**

A pressure history was measured by two piezo-electric pressure gauges (Kastler's 603B) which is shown in Figure2.6. These gauges were flush-mounted on the cylinder surface as shown in Figures 2.7 and 2.8. One is settled near the thrust wall and another is near the outlet of thruster. The pressure history is outputted to an oscilloscope after the amplifier amplifies an output. The amplifier is shown in the right-hand of Figure 2.5.

The pressure history measured near a thrust wall is Figure 2.9. [27] Total

impulsive thrust  $I$  for a single cycle operation is calculated as,

$$I = \int (p - p_0) A dt = (p_4 - p_0) A t_{\text{plateau}} \quad (2.1)$$



**FIGURE 2.5.** Amplifier



**FIGURE 2.6.** Pressure Element

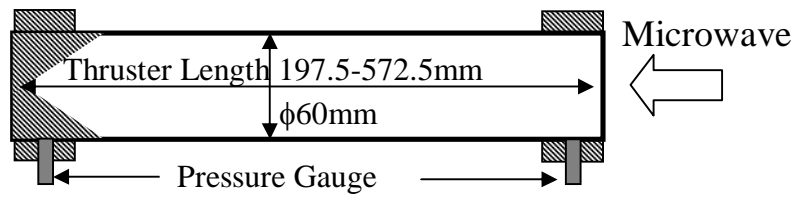


**FIGURE 2.7.** Thruster model with pressure gauge

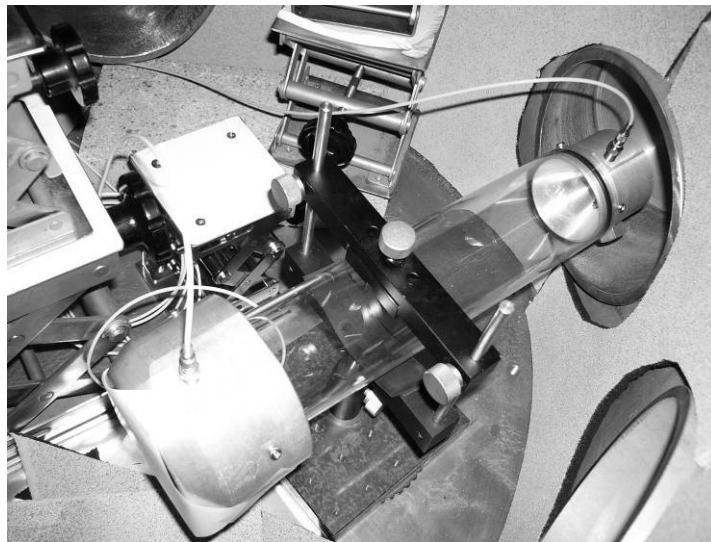


**FIGURE 2.8.** Thruster model with pressure gauge

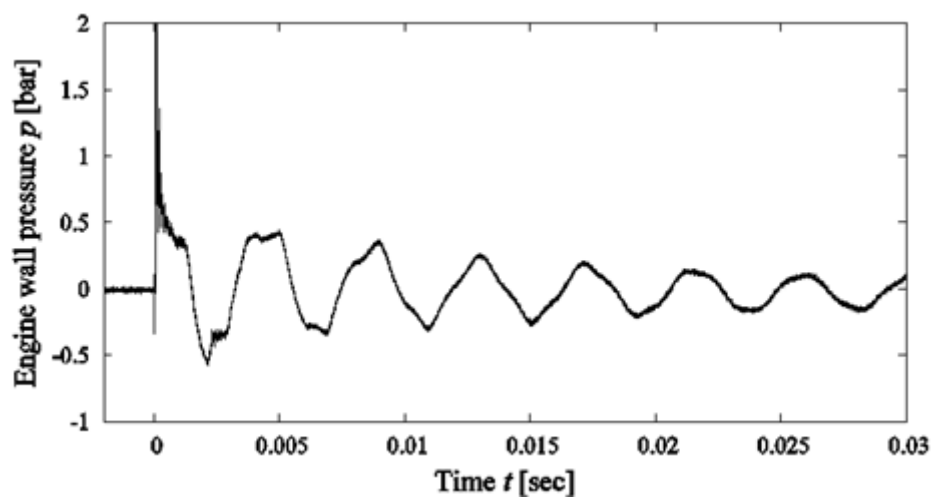


**FIGURE 2.9.** Pressure history at thrust wall by pressure element [27]

## 2.4.2 Load Cell

Thrust was measured by a load cell (Kyowa electronic's KM-10KA) which is shown in Figure 2.10. The measurement system is shown by Figure 2.11. The pendulum whose length is 170mm is used for the thruster moving part. The load cell for measurement is set up so that the thruster is touched by the weight. However, when thrust measurement is conducted by the thrust stand using a load cell, it's necessary to consider the influence of the tube and flow air in the thruster of the forced air-breathing system which is stated in next section. In addition, the waveform is outputted to an oscilloscope after the amplifier amplifies an output. The amplifier is shown in the left-hand side of Fig. 2.5.

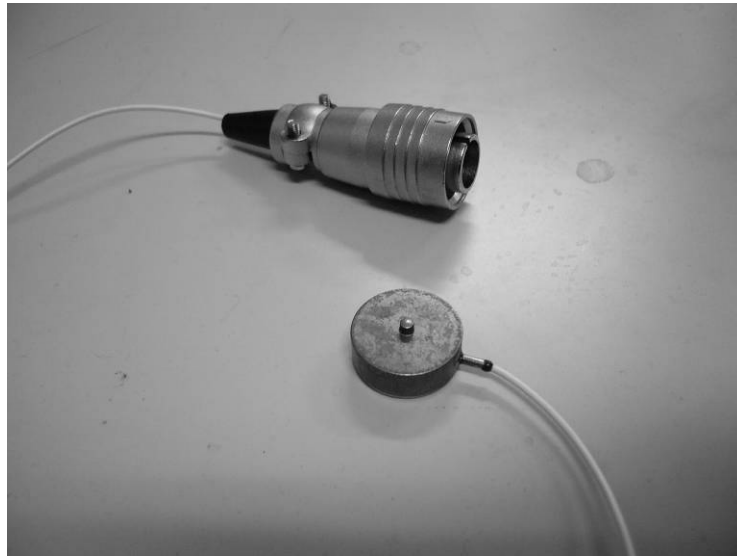


**FIGURE 2.10.** Load Cell

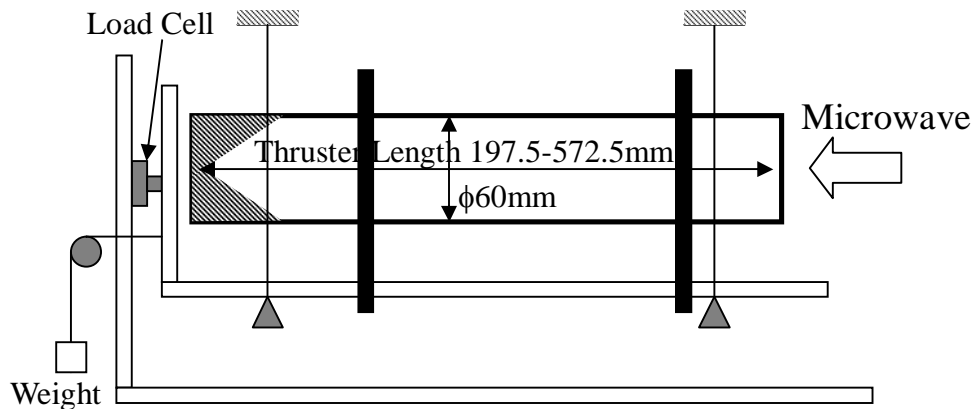


**FIGURE 2.11.** Thruster model with load cell

Here, the calibration method is mentioned. Since this system has low response frequency, it is difficult to calculate a thrust directly from a load cell output. Impulse  $I$  is inputted into the thruster of mass  $M$ , and it begins to move with speed  $V$ , and if the kinetic energy of the thruster is ideally transformed into the energy of the spring in a load cell, it will become as

$$I = MV \quad (2.2)$$

$$\frac{1}{2}MV^2 = \frac{1}{2}kx_{\max}^2 \quad (2.3)$$

$$F_{\max} = kx_{\max} \quad (2.4)$$

Equation 2.5 is derived from Equation 2.2 to Equation 2.4.

$$I \propto \sqrt{\frac{M}{k}}F_{\max} \quad (2.5)$$

Equation 2.5 shows that an input impulse and  $F_{\max}$  have a linear relation. Based on this, the relation of the peak value of an input impulse and a load cell output was investigated. Figure 2.12 shows the relation of the peak value of the load cell output when adding a known impulse to the thrust stand shown in Figure 2.11. Therefore, a calibration can be done from

$$y = 1.2227x \quad (2.6)$$

Here,  $x$  [mV] is the peak value of a load cell output and  $y$  [Ns] is a thrust impulse.

Next, the calibration in the case of microwave repetitive pulse conditions is mentioned. If the response frequency of a system is lowered, it can consider that the generating thrust in the case of microwave repetitive conditions is a steady thrust. And thrust measurement can be done by the steady thrust. The relation of the generating thrust to a load cell output is shown in Figure 2.13. Therefore, a calibration can be done from

$$y = 0.0387x \quad (2.7)$$



Here,  $x$  [mV] is a steady load cell output and  $y$  [Ns] is a thrust. The load cell output measured as a steady thrust is shown in Fig. 2.14. And RF signal at the time of Fig. 2.14 is shown in Fig. 2.15. It turns out that the steady thrust 0.9N is measured after about 0.4 second for which oscillation of the thrust stand is finished.

Last, Comparison of the thrust measurement by a pressure history and a load cell is shown in Figure 2.16. The figure shows that thrust measurement by the pressure history and a load cell can be done in almost comparable precision.

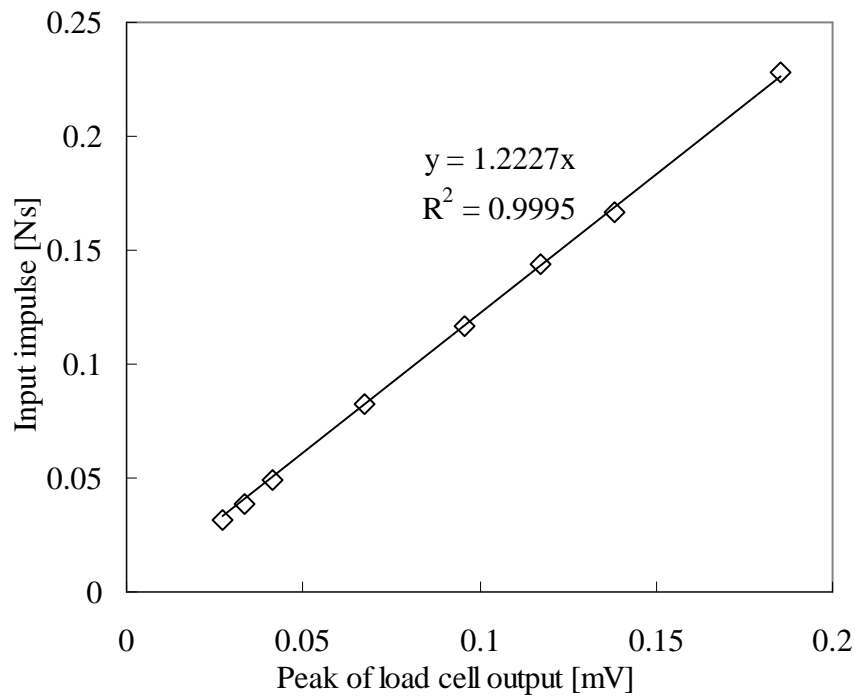


**FIGURE 2.12.** Calibration Result for thrust impulse

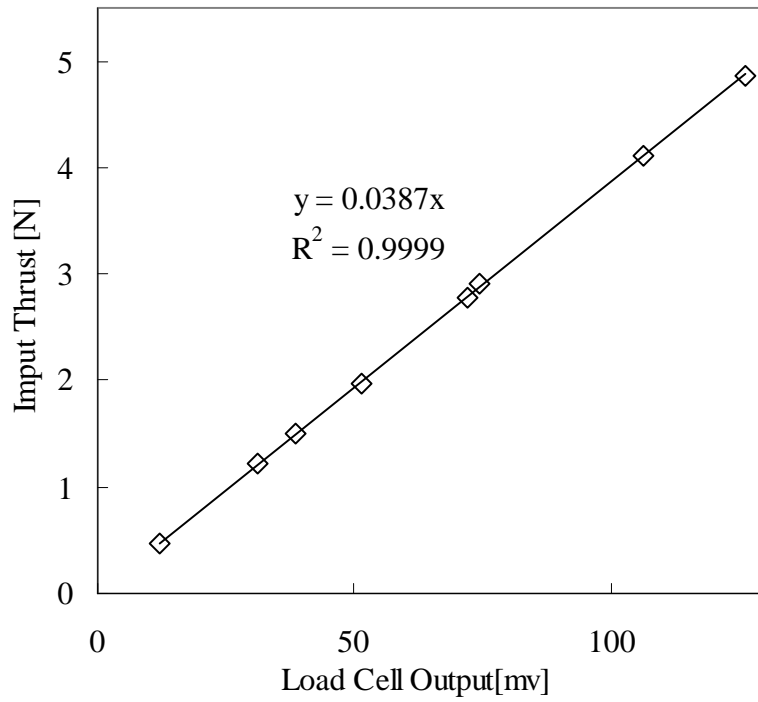


**FIGURE 2.13.** Calibration Result for steady thrust

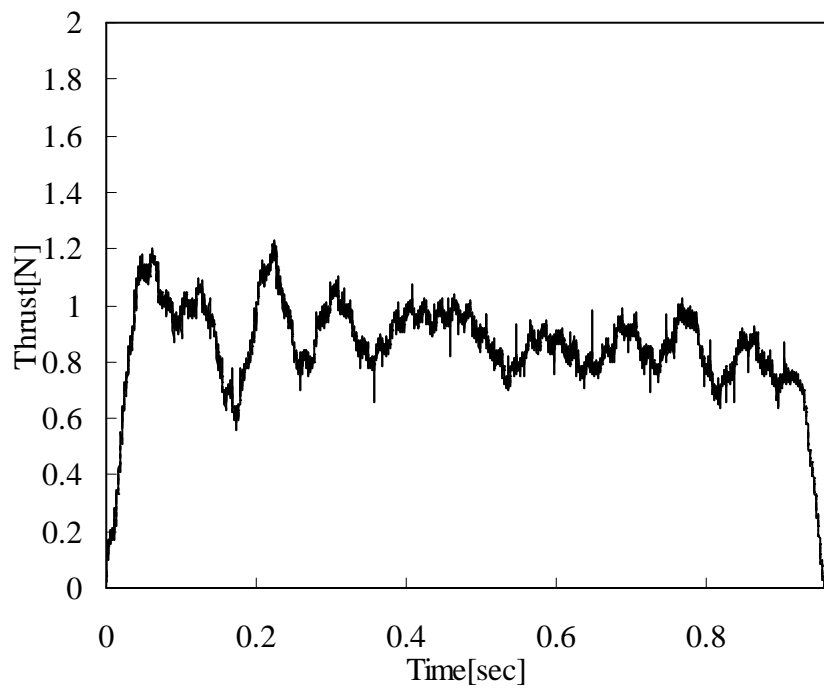


**FIGURE 2.14.** Load Cell Output ( $P=200\text{kW}$ ,  $f=50\text{Hz}$ )

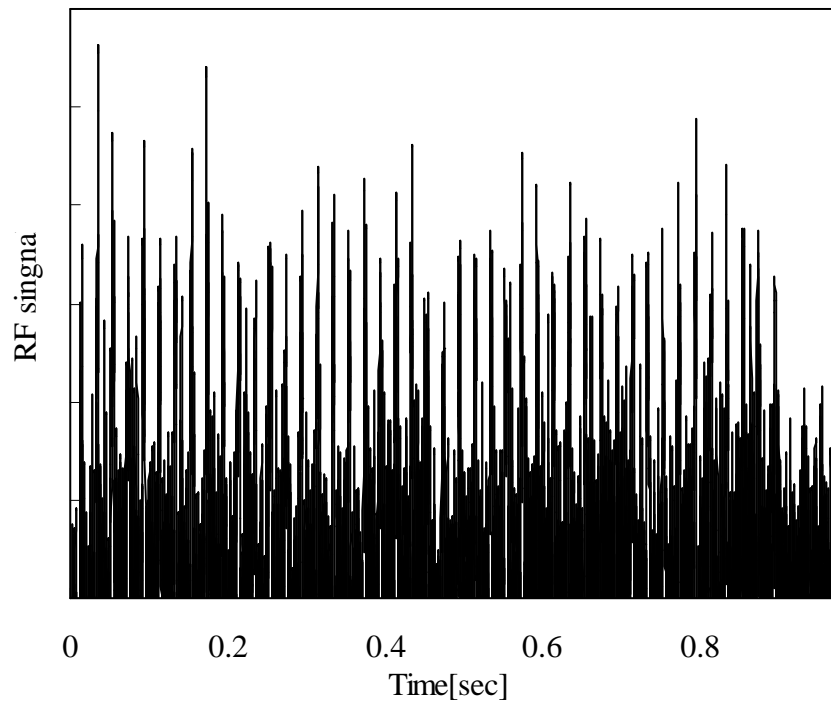


**FIGURE 2.15.** RF Signal ( $P=200\text{kW}$ ,  $f=50\text{Hz}$ )

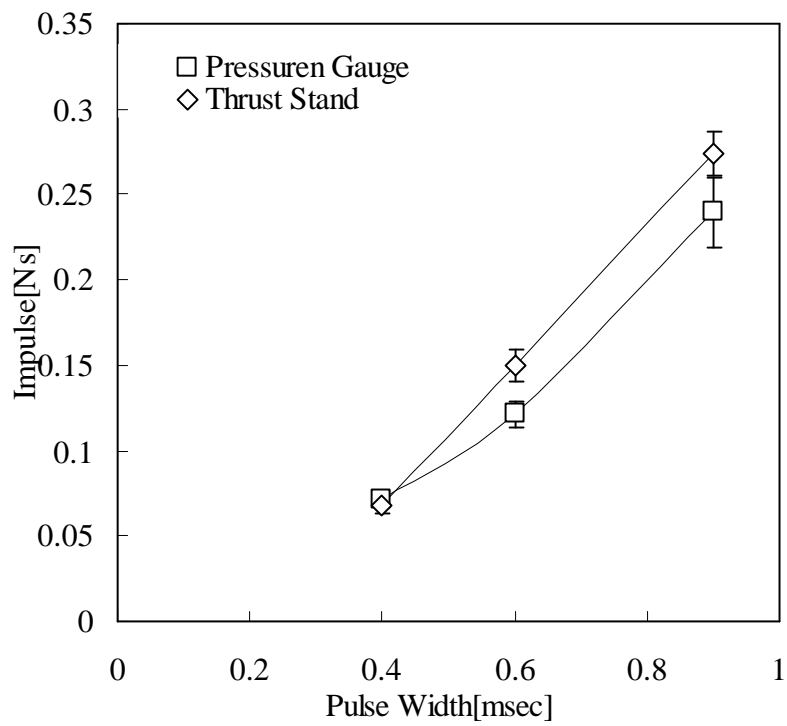


**FIGURE 2.16.** Comparison of thrust measurement of pressure element and load cell

## 2.5 Air-Breathing System

From the past research, when microwave condition is repetitive condition, the thrust was decreased drastically after 2nd pulse. It is already mentioned that the cause is high-pressure gas which remains in a thruster.

In a microwave rocket, ram pressurized air is provided during the high speed flight. For ground facility, instead of ram pressurized air, forced breath system is required to solve these problems. To enhance refilling the new air in the thruster, forced breathing system was built. The system is shown in Figure 2.18. Using a compressor (tank) and valves which are shown in Figure 2.17 pressurized air was induced from thrust wall side of the thruster. The flow velocity was variable by changing the valve number and tank pressure. The tank pressure is kept at 0.4 MPa and the bulk flow velocity  $u_0$  was varied from 2.5 m/s to 10m/s by controlling the number of opening valves.

And the partial filling rate is defined as

$$\frac{\text{Replaced Air Volume}}{\text{Cylinder Volume}} = \frac{V}{LA} = \frac{Au/f}{LA} = \frac{u}{Lf} \quad (2.8)$$

The performance dependence on this parameter was investigated.

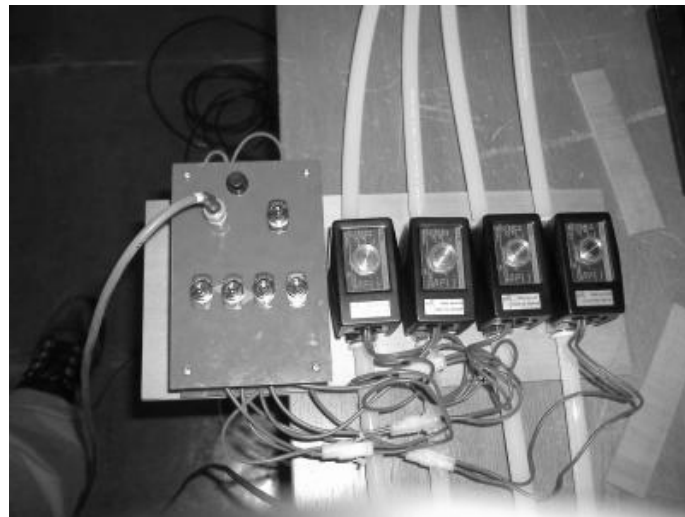


**FIGURE 2.17.** Electric valves for flow operation

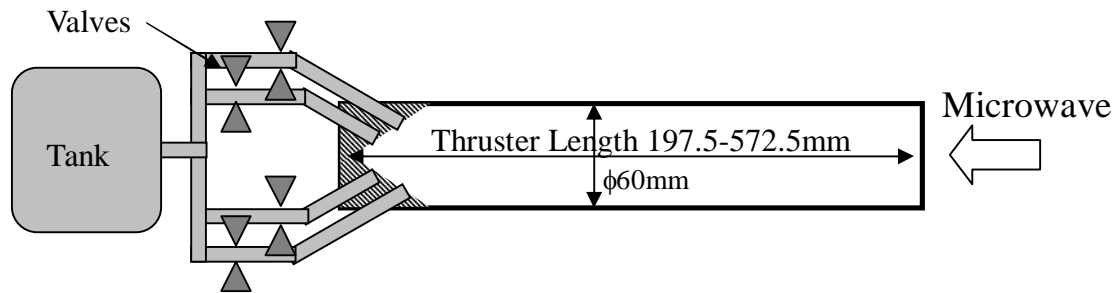


**FIGURE 2.18.** Thruster model with forced air-breathing system

The experiment system which established the thruster model, the pressure element, the load cell, and the forced air-breathing system, is shown in Figures 2.19 and 2.20.

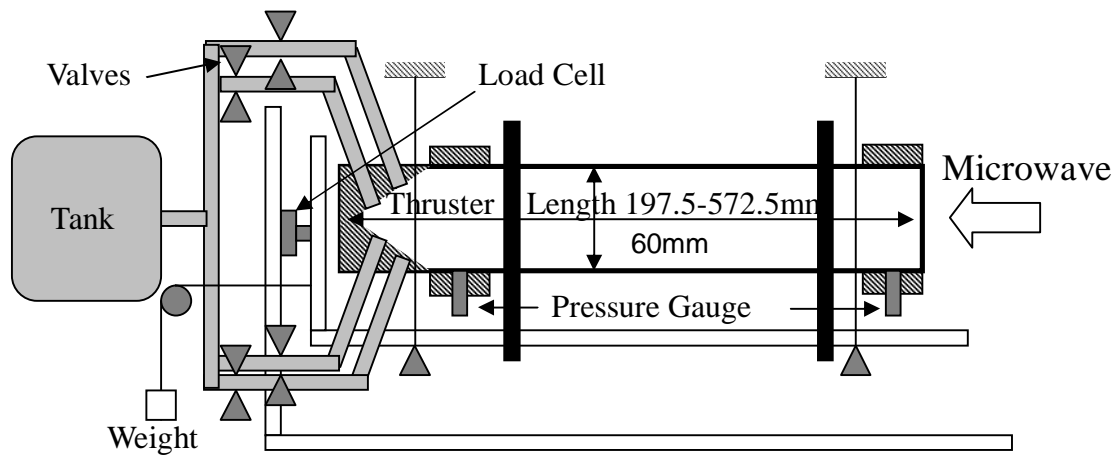


**FIGURE 2.19.** Thruster model with all equipment for experiment

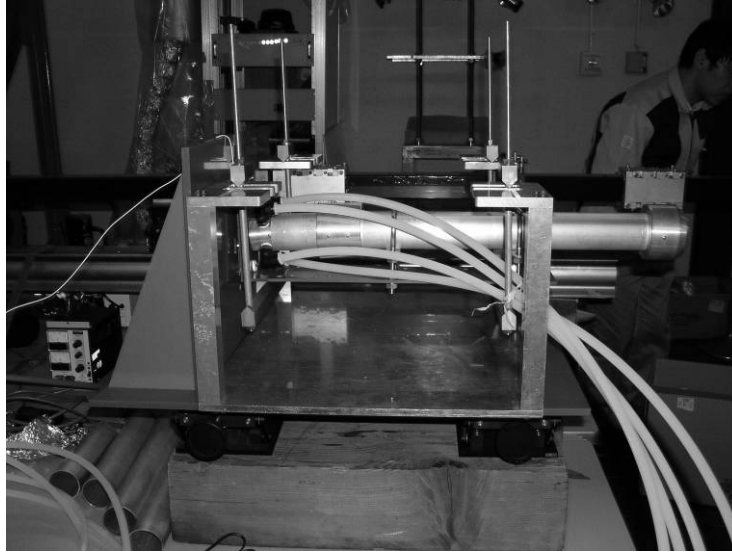


**FIGURE 2.20.** Thruster model with all equipment for experiment

## 2.6 Chamber

In assuming an actual flight, when a microwave rocket flies by high altitude, an atmospheric pressure decrease by altitude. And, the pressure in a thruster also decreases. Therefore, the pressure dependability of a thrust is also one of the important components in the viewpoint of thrust optimization of a microwave rocket.

In this research, the chamber as shown in Figure 2.21 was used in order to assume thruster dependence on pressure in the thruster. This chamber is 500mm in diameter, and 250mm in height. Microwave was entered horizontally from chamber window. Measurement of the thrust and propagation velocity of ionization front in the decompression air condition of 1atm to 0.001atm was done, and plasma structure was observed. Air, a helium, argon, and nitrogen were used for the gas species in a chamber. In addition, only a pressure element is used for thrust measurement in the chamber.

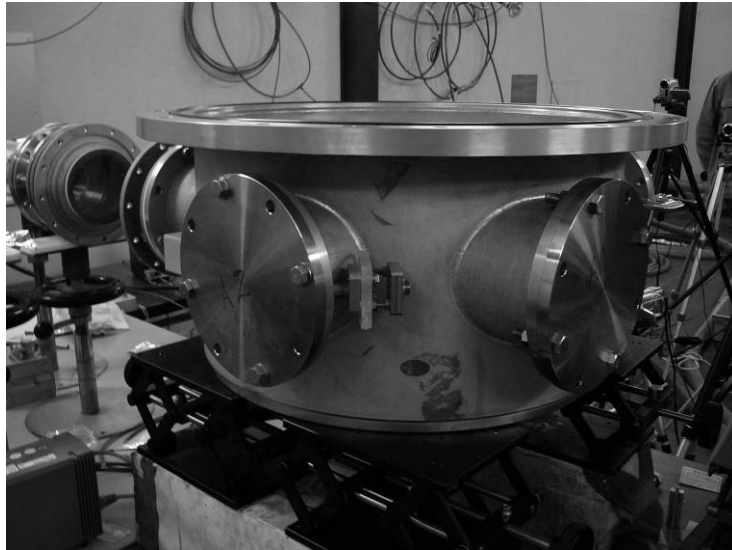


**FIGURE 2.21.** Chamber

## **2.7 High Speed Camera**

High speed camera (FASTCAM Ultime 40K (made by Photron)) was used for photography of the ionization wave front which propagates in the thruster. The ionization wave front was observed, and propagation velocity of the ionization front was measured by it. Frame speed was set up with per second 40500.

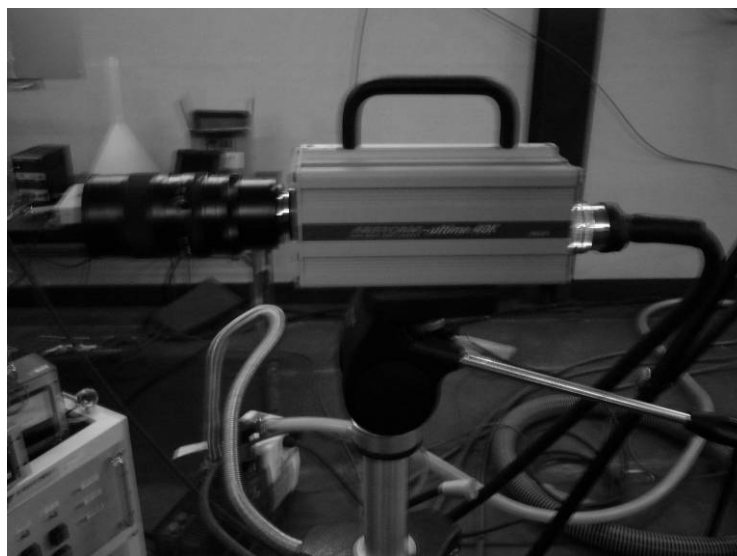


**FIGURE 2.22.** High Speed Camera

## Chapter 3

### Single Pulse Condition

There are a microwave condition, a thruster condition, atmospheric conditions and so on as a component to determine the thrust of a microwave rocket. In this chapter, on the single pulse conditions of microwave, pulse width, thruster length, pressure in the thruster, gas species and so on were changed, and the optimal thrust conditions were verified on each conditions. And thrust optimization is achieved for design of microwave rocket.

#### 3.1 Pulse Width and Thruster Length

Measurement of the thrust impulse by load cell was conducted for the power range of 470-840kW. The measured thrust impulse was plotted on Figure3.1.

When the pulse duration is smaller than a certain condition, the impulse increases with increase of pulse duration. Indeed the increment of impulse is saturated and the maximum impulse for each thruster is obtained when exceeds the condition. The maximum condition has dependence on the thruster length  $L$ . The maximum is obtained when the traveling length of the ionization front  $U_{ioniz}$  is identical to  $L$ .

Momentum coupling coefficient dependence on pulse width of microwave is shown in Figure3.2, and momentum coupling coefficient dependence on normalized plasma length is shown in Figure3.3. When thrust is max value, momentum coupling coefficient used as the index of thrust performance didn't become max value. When normalized plasma length is about 0.6 and plasma has detailed structure, momentum coupling coefficient which is used as the index of thrust performance became max value. In addition, the maximum of momentum coupling coefficient has max value when pulse width is very short in MSC region which doesn't have detailed structure of plasma. The momentum coupling coefficient in the condition is shown in Figure 3.4. In a MSC region, it is considered that the ionization wave front and a shock wave separate and energy conversion is not done efficiently. Chapter3.4 discusses the details about a region.



As mentioned above, the condition selection as choosing thrust performance or thrust value for design of microwave rocket can be archived.

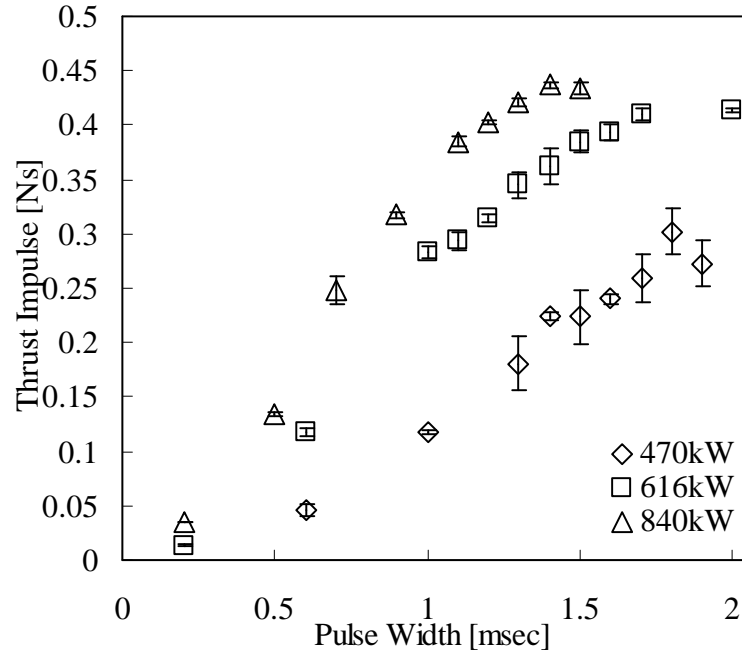


**FIGURE 3.1.** Thrust impulse dependence on pulse width; L=590mm

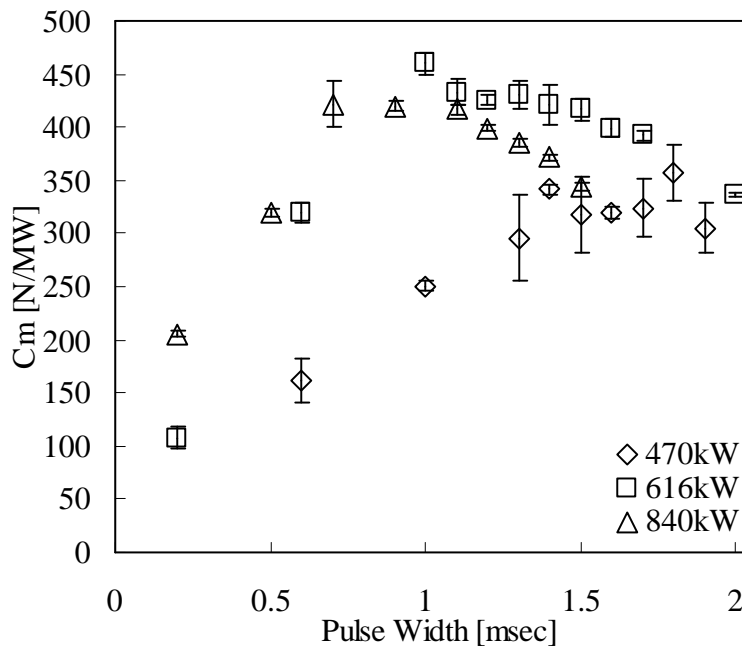


**FIGURE 3.2.** Momentum coupling coefficient dependence on pulse width; L=590mm

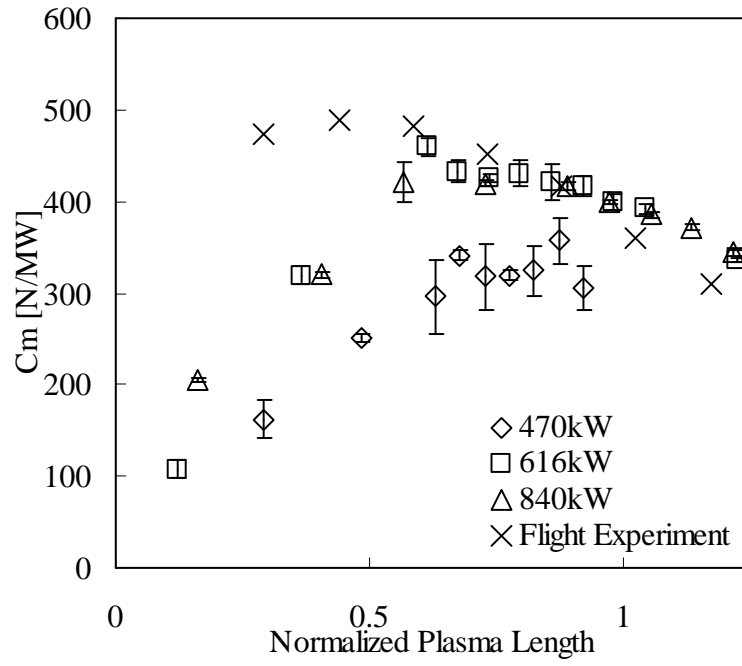


**FIGURE 3.3.** Momentum coupling coefficient dependence on normalized plasma length;  $L=590\text{mm}$

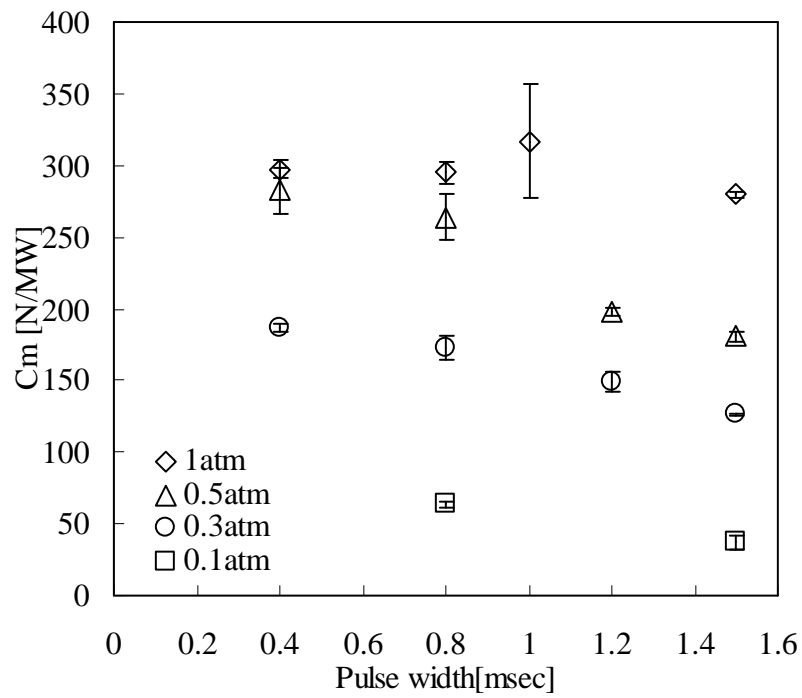


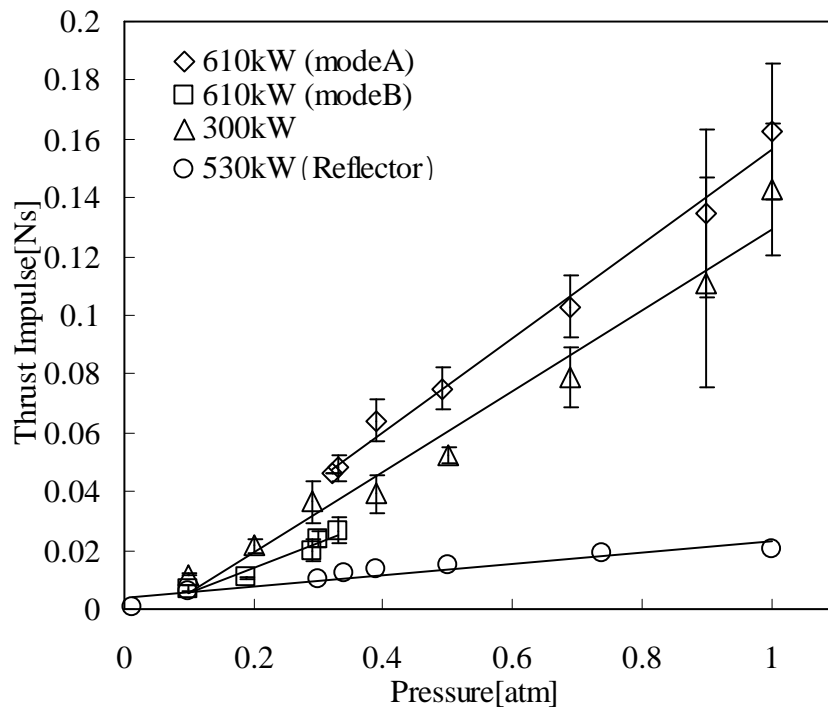
**FIGURE 3.4.** Momentum coupling coefficient dependence on pulse width at each ambient pressure;  $L=300\text{mm}$

## 3.2 Pressure in the Thruster

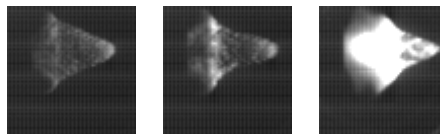
Measurement of the thrust impulse at various pressure in the thruster was conducted for the power range of 300-610kW. The measured thrust impulse was plotted on Figure 3.4. And, pulse width was set to the length that a thrust is obtained most.

Figure 3.5 show that a generating thrust has linear relations in ambient pressure. And, the filament structure of plasma was confirmed as shown in Figure 3.6 (a) and (b) in mode A, and the filament structure of plasma has disappeared as shown in Figure 3.6 (c) in mode B. That is, it turns out that the value of a generating thrust decreases greatly, when the filament structure of plasma disappears.

It is suggested that the filament structure of plasma has contributed to the generating thrust greatly and depends on pressure.



**FIGURE 3.5.** Thrust Impulse dependence on pressure in the thruster; L=100, 300mm



**FIGURE 3.6.**(a),(b),(c) The high speed camera photograph of plasma  
( Atmosphere pressure:1.0atm, 0.5atm, 0.1atm )

### 3.3 Microwave Electric Power

It turns out that thrust increases according to the increment in microwave power as shown in Figure 3.5, even if pressure in the thruster was same.

Here, momentum coupling coefficient dependence on the pressure in the thruster is shown in Fig. 3.7. When microwave electric power was 530kW and 610kW and pressure in the thruster was more than a certain steady pressure, Momentum coupling coefficient maintains about 350. However, momentum coupling coefficient is decreasing, when pressure in the thruster was less than a certain steady pressure. And when microwave electric power is 300kW, even if pressure in the thruster is 1 [atm], momentum coupling coefficient wasn't a steady value and decrease according to a decline in pressure. Furthermore, when the momentum coupling coefficient was the steady value, detailed structure was confirmed in the ionization front which propagates in the thruster as shown in Fig. 3.6 (a) and (b). On the other hand, when a momentum coupling coefficient wasn't a steady value, the detailed structure of the ionization front had disappeared as shown in Fig. 3.6 (c).

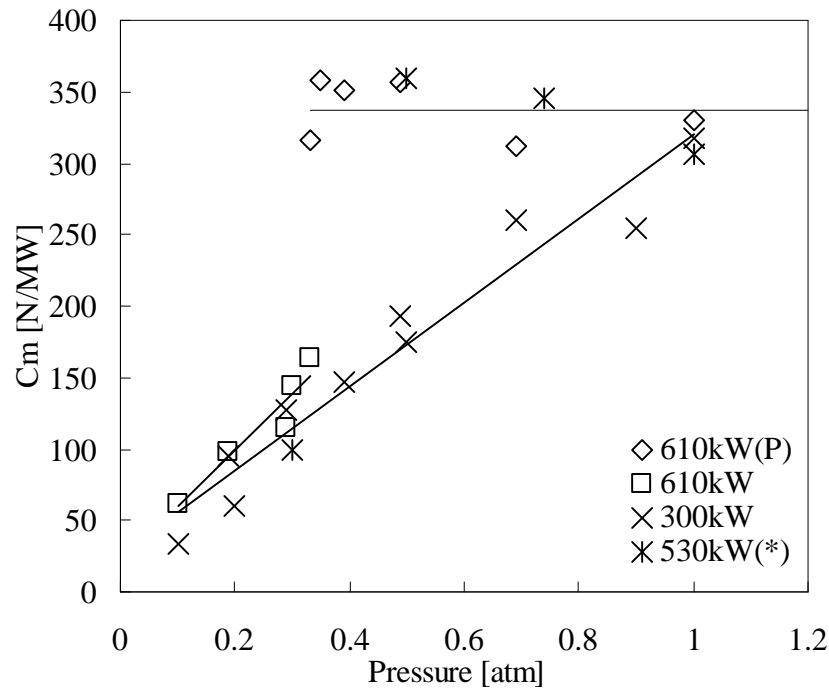


**FIGURE 3.7.** Momentum Coupling Coefficient dependence on pressure in the thruster; L=300mm

As mentioned above, it is suggested that the filament structure of plasma depend on microwave electric power.

### 3.4 Dependency on Pressure and Microwave Power

In order to investigate the relation of the thrust performance by a pressure in the thruster and microwave power, the condition of ionization front propagation, and a pressure in the thruster and microwave electric power density were summarized (refer to appendix). It evaluate by microwave electric power density, because plasma structure depende on microwave power density.

The 3D graph which microwave electric power density is set for the axis of ordinate, and microwave power density and pressure in the thruster is set for the horizontal axis is shown in Fig. 3.8 based on Fig. 3.7. In addition, the value predicted from the tendency is also included. Fig. 3.8 shows that the value of a momentum coupling coefficient is optimized, when microwave power density and atmosphere pressure is more than a certain value. And, it is turned out that the momentum coupling coefficient decreases drastically as atmosphere pressure or microwave power density decreases, when less than the condition.

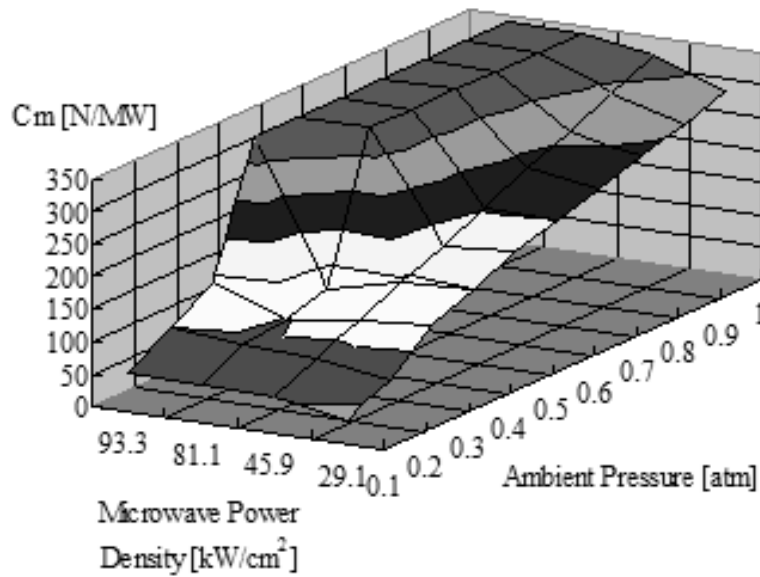


**Figure 3.8.** Momentum coupling coefficient dependence on pressure in the thruster and microwave power density

Furthermore, the boundary of the region where the filament structure is appeared and the region where filament structure is disappeared shown by appendix almost overlap with the boundary where the momentum coupling coefficient is optimized by Figure 3.8.

Here, each region and the cause of the region change is considered. Figure 3.9 shows the ionization front propagation velocity and shock wave propagation velocity in the conditions of microwave electric power density 46-93 kW/cm<sup>2</sup> and atmosphere pressure 0.1-1.0atm. The shock wave drive by microwave plasma is reproduced using the Computational Fluid Dynamics simulation (CFD) by Shibata et al. It is clear by CFD that change occurs in the pressure-distribution structure of the shock wave back by the difference of ionization front propagation velocity. When ionization wave front propagation velocity is late as subsonic, a shock wave turns into a vertical shock wave, and is departed and propagated ahead a heating region. This condition is called Microwave Supported Combustion (MSC). On the other hand, if ionization wave front propagation velocity is the supersonic speed exceeding M2, a heating region and a shock wave is in agreement and propagate. This condition is called Overdriven Microwave Supported Detonation (Overdriven MSD). [22]

Therefore, it is a MSC region in the condition of microwave power density 46 kW/cm<sup>2</sup>, since ionization front propagation velocity differs from shock wave propagation velocity greatly from Figure 3.8. And it is a C-J MSD region in the condition of microwave electric power density 93kW/cm<sup>2</sup> and more than 0.3 [atm] of pressure in the thruster not a MSC region or an Overdriven MSD region.

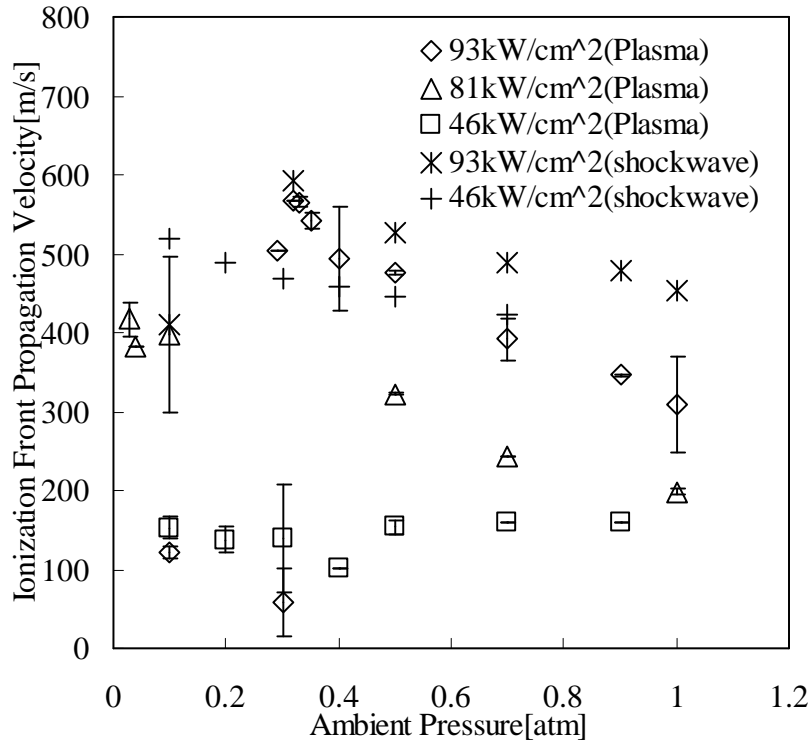


**Figure 3.9.** Ionization front propagation velocity and shock wave propagation velocity dependence on pressure in the thruster  
(Plasma: ionization front propagation velocity,  
shockwave: shock wave propagation velocity)

The value in the pulse width conditions which can obtain the highest momentum coupling coefficient on each condition becomes important for the design of microwave rocket. The predicted 3D graph show maximum value of momentum coupling coefficient dependence on pressure in the thruster and microwave power density by Figure 3.8 and the tendency of the momentum coupling coefficient by the pulse width change on each condition is shown in Fig. 3.10.

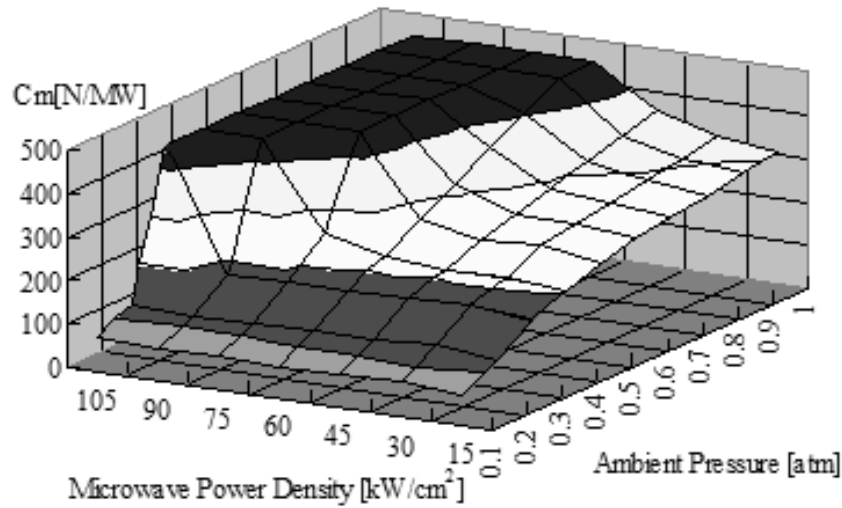


**Figure 3.10.** Maximum value of momentum coupling coefficient dependence on pressure in the thruster and microwave power density ( prediction)

The conditions of microwave power density and pressure in the thruster which the optimal thrust performance is obtained is founded by Figure 3.10. For example, when the microwave electric power density is low, high atmosphere pressure is required in order to obtain the optimal thrust performance. And, when the pressure in the thruster is low, high microwave power density is needed for optimal thrust performance.

### 3.5 Thrust Performance by Gaseous Species

When a microwave rocket flies in rocket mode, the gaseous species of the fuel are also one of the important components. Air, a helium, nitrogen, and argon were used as gaseous species. But luminescence of the sapphire window of the chamber was confirmed in the conditions that the pressure in a chamber is low, or the conditions that microwave electric power is high. The luminescence is electric discharge. Thus, power was not supplied appropriately in a thruster, and experiments were not able to conduct not much. The contents which are suggested from a few measurement results are explained. In addition, in order to prevent luminescence of the sapphire window of a chamber, it is thought effective to construct a system which makes low microwave



power density to pass the chamber window using optical system.

It is turned out that a thrust almost equal in the case of the same power and pulse width conditions is obtained as shown in Figure 3.11. And, it is found that the value of a thrust decreases according to a decline of pressure in the thruster and microwave pulse width like the condition of air.

In order to compare thrust performance, the graph of the momentum coupling coefficient is shown in Fig. 3.12. "The optimal thrust performance can be obtained with a certain pulse width" and "If pulse width with a certain optimized pressure is given, steady thrust performance is maintained" are confirmed like the case of air as shown in Fig. 3.12. As mentioned above, "Even if gaseous species change, it has the above tendencies", "Contribution of nitrogen is large in the component of air" and "The maximum of a momentum coupling coefficient contributes to molecular weight (Fig. 3.13 also discusses)" is suggested.

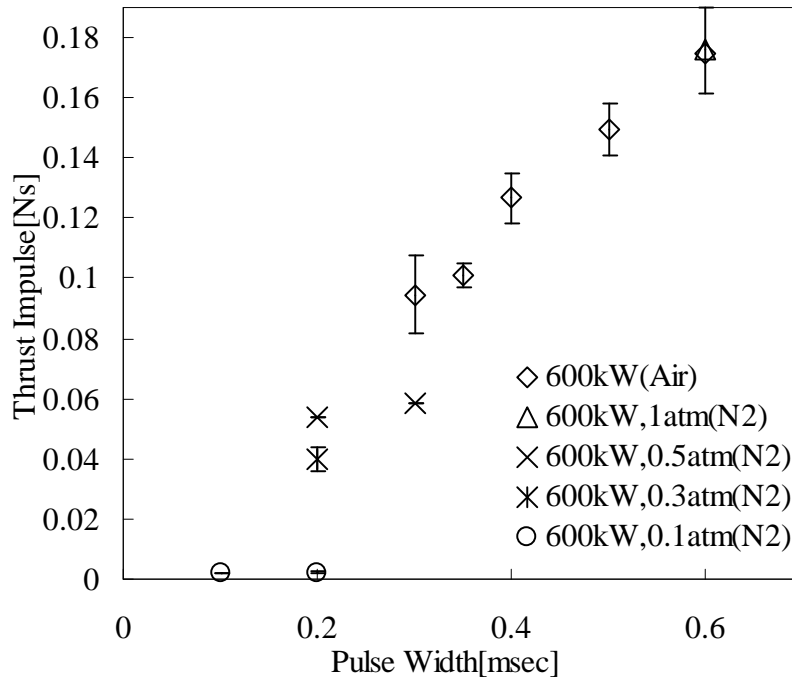


**FIGURE 3.11.** Thrust Impulse dependence on Pulse width at each ambient pressure ( $\phi 60$  parabola reflector+ Rectangle tube(L=320mm))

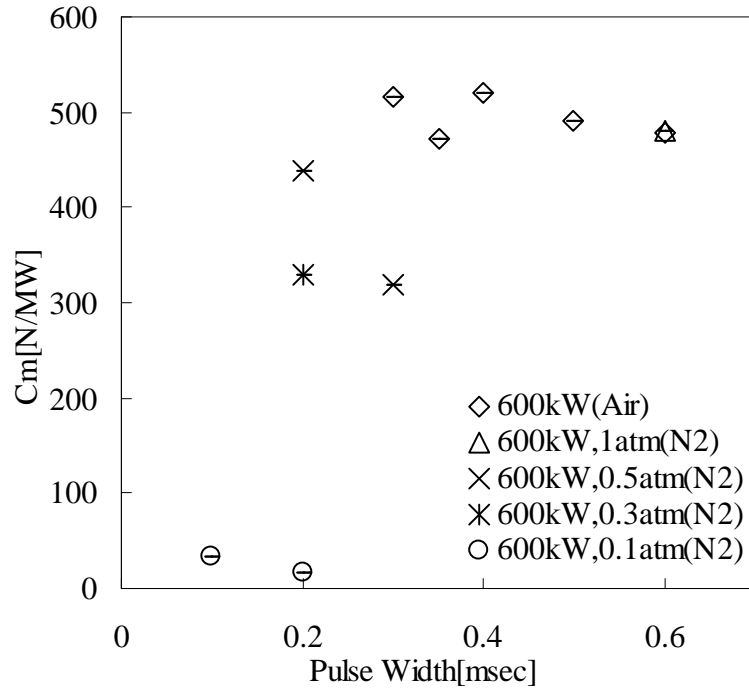


**FIGURE 3.12.** Momentum coupling coefficient dependence on pulse width at each ambient pressure

Although a thruster model is consist of parabola reflector without tube and calculation of a momentum coupling coefficient is difficult, it is suggested that thrust has dependence on pressure in the thruster like the case of air and nitrogen.

And, on the conditions of microwave electric power 600[kW] and pressure in the thruster 1[atm], the propagation velocity of the ionization front is less than 1000[m/s] in the case of a helium, 2-5000[m/s] in the case of argon and more than 500[m/s] in the case of nitrogen, and each molecular weight is helium 4.00, argon 39.95, and nitrogen 28.01. Furthermore, it is thought that electric power density is quite high, sufficient conditions for plasma to ignite, since it is only a parabola. As mentioned above, it is suggested that momentum coupling coefficient has dependence on molecular weight. Furthermore, although the ionization voltage of a helium, oxygen, and nitrogen differs from 12.2-24.58[V] by Table 3.1, it doesn't depend on the ionization voltage. [24] Therefore, it's suggested that momentum coupling coefficient has dependence on molecular weight, when satisfying optimization conditions. It's because sonic speed

becomes fast and specific impulse becomes large when molecular weight becomes small. That is, thrust will become large if molecular weight becomes large. On the other hand, when molecular weight becomes small, though thrust becomes small, specific impulse becomes large.

But microwave power density is very high since this experiment is conducted to use only parabola reflector. And, experiment counts are not enough and only stable gaseous is used. Therefore, it is necessary to conduct the further experiment in order to optimize the thrust by gaseous species change such as using gaseous which is possible to use in real flight like hydrogen and has big difference of physical properties. And, it is thought that it is necessary to consider only molecular weight in selection of gaseous species, if it will assume that it depends for a momentum coupling coefficient on molecular weight and optimization conditions are satisfied. But the speed of the ionization front and ionization voltage differs greatly in fact. Therefore, it is required to determine the gaseous after verifying about the difference in the physical properties by gaseous species.

**Table1 3.1** Gaseous ionization voltage [24]

Gas Species	Ionization Voltage[V]		Gas Species	Ionization Voltage[V]
He	24.58		H <sub>2</sub>	15.44
Ne	21.55		O <sub>2</sub>	12.2
Ar	15.75		N <sub>2</sub>	15.58
Kr	13.96		K	4.33
Xe	12.12		Cs	3.87
Hg	10.42			

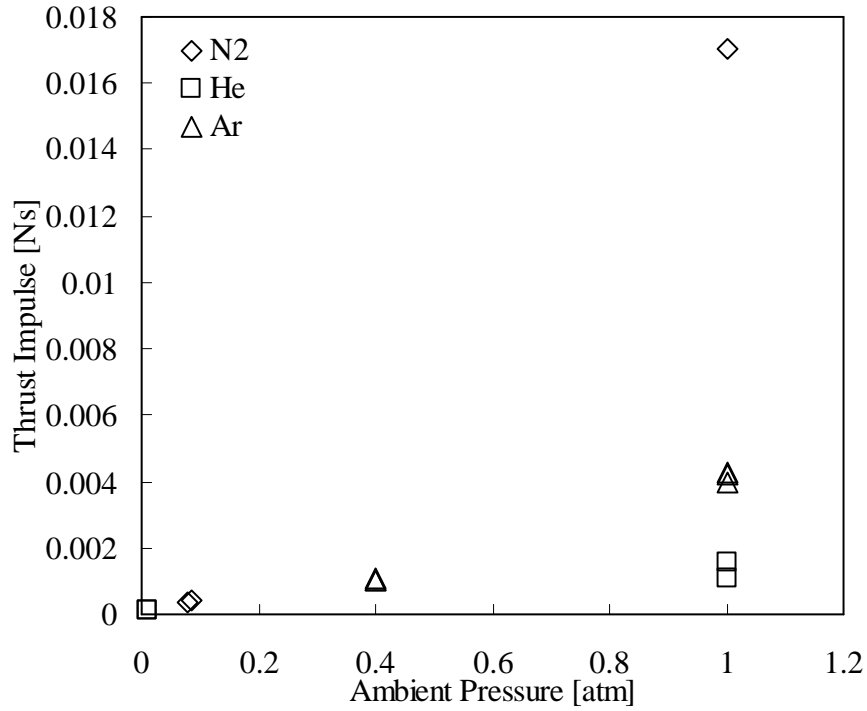


**FIGURE 3.13.** Thrust Impulse dependence on Pulse width at each ambient pressure  
( parabola reflector )

### 3.6 Conclusion of Single Pulse Condition

The conditions to obtain the optimal thrust of the single pulse of microwave were verified by changing pulse width, thruster length, pressure in the thruster, gas species and so on and . It turned out that there are conditions which can obtain the maximum thrust and the most efficient thrust performance on each condition. From these results, the conditions can be determined to obtain the most efficient thrust performance or the maximum thrust in the limited conditions. As mentioned above, it became possible to optimize the thrust of the microwave rocket in microwave single pulse conditions. In the following chapter, it is verified about the thrust optimization in microwave repetitive pulse condition.

## Chapter 4

### Multi-Pulse Condition

In addition to conditions in microwave single pulse such as pulse width, thruster length pressure in the thruster and gas species were verified by Chapter3, there are conditions in microwave repetitive pulse. A thrust decreases drastically after 2nd impulse in the condition of microwave repetitive. The cause is that the hot gas is remained in a thruster. In order to solve this, the forced air-breathing system is developed assumed front air-breathing at the time of a microwave rocket flight. In this chapter, the influence on the thrust by a forced air-breathing system is verified mainly.

#### 4.1 Thrust Recovery by Partial Filling Rate

The thrust impulse for each pulse count is shown in Figure 4.1. The result with the maximum flow rate case  $u_0=10\text{m/s}$  was compared to the result without air flow. In the case of no flow, the impulse decreased with the pulse counts. On the other hand, in the case of  $u_0=10\text{m/s}$ , thrust impulse was slightly decreased at the second pulse. However, almost steady thrust impulse was obtained at the 3rd pulse and further.

Therefore, the thrust impulse maintained after second pulse was regarded as the steady impulse in this study.

#### 4.2 Impulse Dependence on $u_0$ and $f$

The steady impulses in the repetitive pulse operations  $f=20\text{Hz}$  and  $50\text{Hz}$  are plotted in Figure 4.2.  $P$  was kept at  $300\text{kW}$  with  $L=390\text{mm}$ . When  $u_0=10\text{m/s}$ , the steady impulses were almost identical at both repetitive frequencies. However, at  $f=50\text{Hz}$  the steady impulse decreases with the decrease in  $u_0$  at  $7.5\text{m/s}$  and further, while the impulse was kept high in the range  $5\text{m/s} \leq u_0 \leq 10\text{m/s}$  at  $f=20\text{Hz}$ . It suggests that when the pulse repetition frequency is high, the interval time between the pulses is too short and filled fresh air not sufficient to have full impulse recovery.

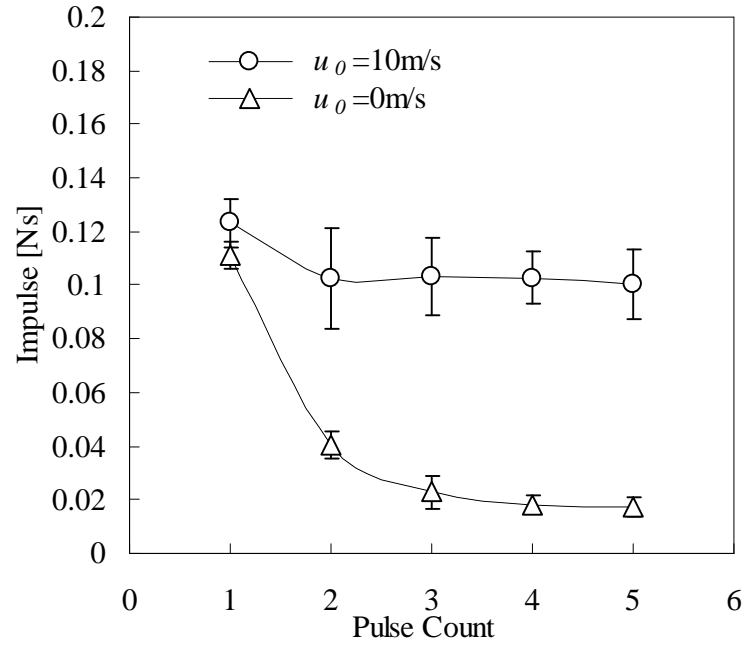


**FIGURE 4.1.** Thrust impulse for each pulse count in repetitive pulse operations.  
 $f=50\text{Hz}$  and  $L=390\text{mm}$

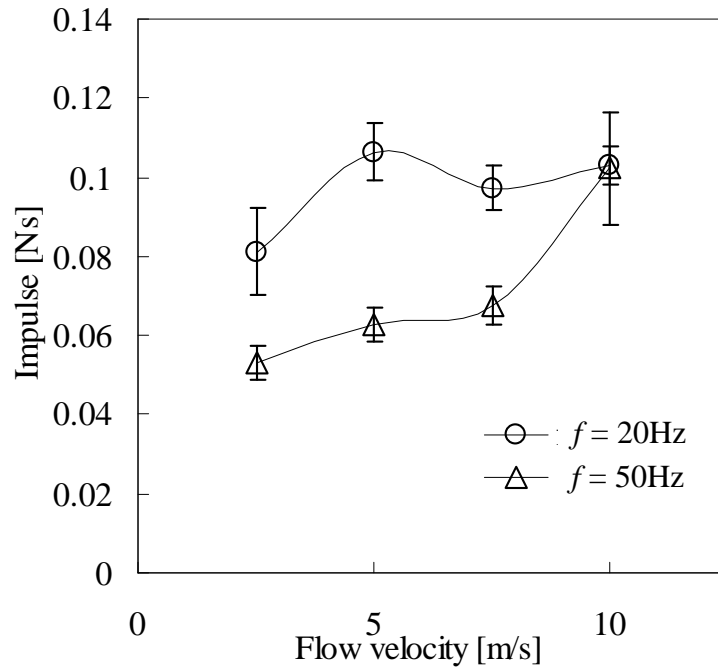


**FIGURE 4.2.** Steady impulse for various  $u_0$  and pulse repetition frequencies  
 $P=300\text{kW}$ ,  $L=390\text{mm}$

### 4.3 Dependence on the Partial Filling Rate

In this sub-section, the filling condition is characterized using the partial filling rate. Measured thrust impulse normalized by the impulse at the first pulse  $I/I_{single}$  are plotted as a function of the partial filling rate in Figure 4.3. [28]

The predictions by the analytical engine cycle model described are also plotted by a solid line in the figures. [25] The measurements and computations showed a good agreement. It would be concluded that the Microwave Rocket can operate in a repetitively pulsed mode without performance degradation when the partial filling rate is kept larger than unity.

However, there are the conditions that the measurements and computations didn't show a good agreement. This is explained in the following section.

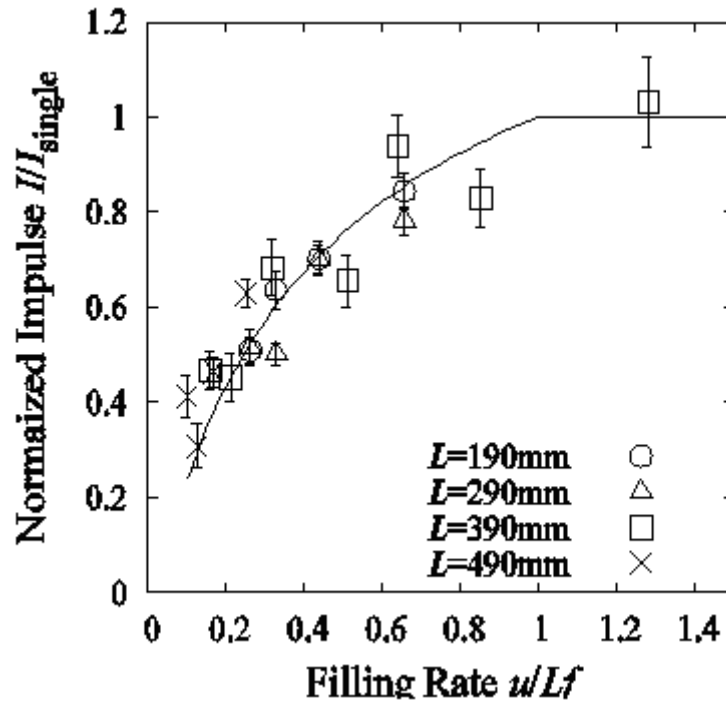


**FIGURE 4.3.** Thrust impulse dependence on the partial filling rate; Symbols show measurements and a solid line does theoretical prediction. Steady impulse for various  $u_0$  and pulse repetition frequencies [28]

## 4.4 Contribution of Plasma Length in Low Partial Filling Rate Region

In the foregoing paragraph, thrust is evaluated in order to obtain a high thrust, when normalized plasma length is about 1 which means plasma length to be almost equal to thruster length. The experiment was conducted by changing normalized plasma length in order to evaluate the influence of a partial filling rate. The thrust dependence on partial filling rate is shown in Fig. 4.4. The important experimental condition is summarized in Table 4.1.

It turns out that sufficient flow velocity in a thruster causes thrust recovery like Figure 4.3. But a partial filling rate does not fit a solid line in less than partial filling rate 0.3. The plasma length normalized by thruster length was about 0.5 in this region.  $L_{thruster}$  is rewritten as plasma length  $L_{plasma}$  when partial filling rate  $u/L_{thruster}f$  becomes shorter than normalized plasma length (partial filling length  $u/Lf <$  normalized plasma length  $l$ ), it becomes as shown in Figure 4.5.

It is found from Figure 4.5 that the measurements and computations showed a good agreement. Therefore, it turned out that the influence of plasma length becomes large more than thruster length for forced air-breathing at the time of partial filling length  $u/L_{thruster}f <$  normalized plasma length  $l$ . The cause is considered that the remained hot gas in a thruster has only a part of plasma length in the case of partial filling length  $u/L_{thruster}f <$  normalized plasma length  $l$ .

As mentioned above, partial filling rate evaluated by  $u/L_{thruster}f$  in the case of partial filling length  $u/L_{thruster}f >$  normalized plasma length  $l$  and partial filling rate evaluated by  $u/L_{plasma}f$  in the case of partial filling length  $u/L_{thruster}f <$  normalized plasma length  $l$ . The cause is considered that the remained hot gas in a thruster has only a part of plasma length in the case of partial filling length  $u/Lf <$  normalized plasma length  $l$ .



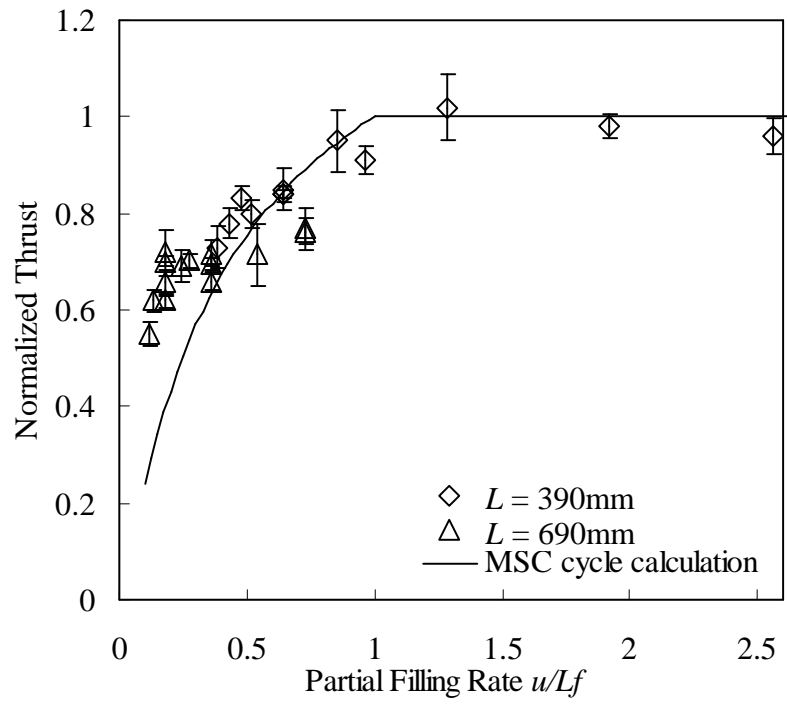


**FIGURE 4.4.** Normalized thrust dependence on partial filling rate

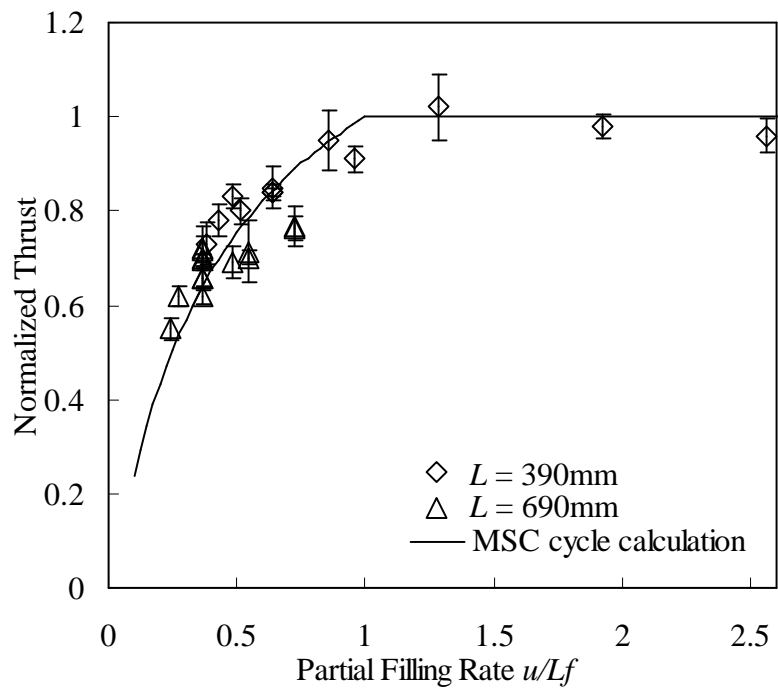


**FIGURE 4.5.** Normalized thrust dependence on partial filling rate (evaluated by  $l$ )

Table 4.1 Experimental Conditions

Thruster Length $L$ [mm]	Pulse Width $\tau$ [msec]	Normalized Plasma Length $l$
390	2.6	Almost 1.0
690	1.3	Almost 0.5

## 4.5 Self Air-Breathing

Thrust dependence on partial filling rate is verified by the foregoing paragraph. Here, when a partial filling rate is 0 which mean no forced air-breathing system, the thrust value is interesting again. Figure 4.6 show 2nd thrust impulse with no forced air-breathing at various microwave repetitive frequency.

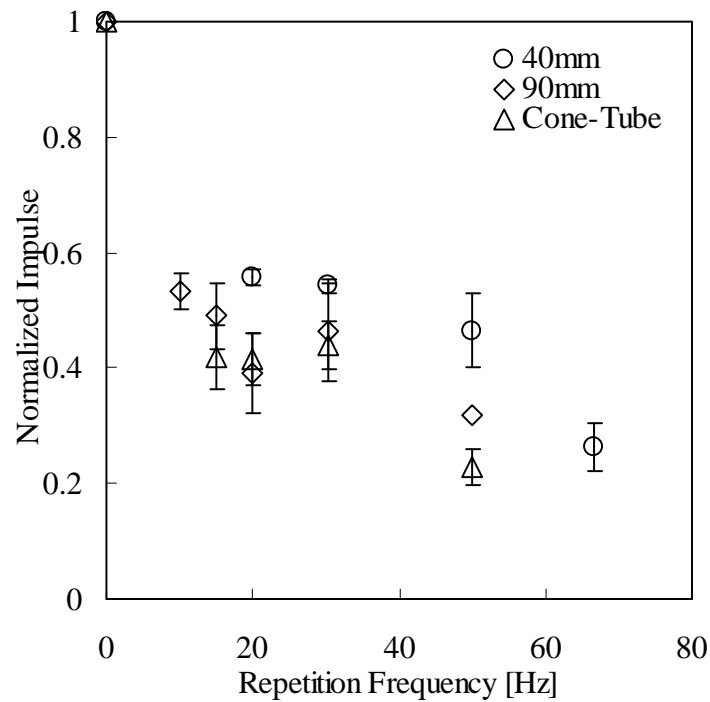
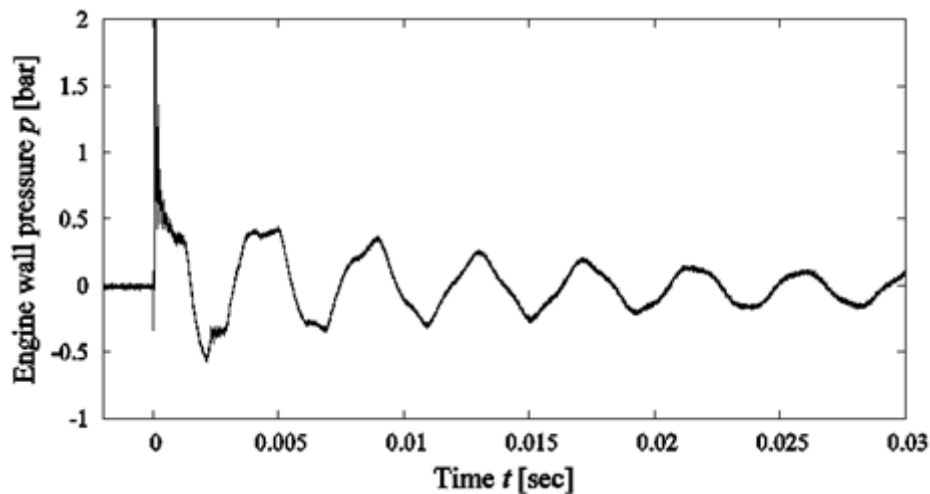


FIGURE 4.6. 2nd thrust impulse with no forced air-breathing

It turns out that normalized thrust becomes 0.2 to about 0.6, although it has some difference by thruster form from Figure 4.6. And, the value doesn't approach 0. Figure 4.7 shows the pressure history near a thrust wall. [27] It turns out that pressure oscillation has occurred after 0.002sec. It is suggested that the negative pressure occurred in the thruster by this pressure vibration and some natural air-breathing has occurred.



**FIGURE 4.7.** Pressure history at thrust wall by pressure element [27]

Thrust decrease become restrictive by the natural air-breathing, although it has some difference by thruster from.

And, it is also known that the maximum of the microwave repeat frequency which can acquire the effect of natural air-breathing by observing the pressure oscillation for each pulse. (About 200Hz is a maximum since one pressure oscillation is 0.005sec In the case of Fig. 4.7.) If it becomes the repeat frequency beyond it, it is thought that the thrust is decreased drastically.

As mentioned above, it is traded off to obtain thrust recovery by establishing mechanisms such as a front air intake or to accept decreased thrust in stead of not to establish in the case of the design of a microwave rocket. From now on, verification of the maximum of microwave repetitive frequency, optimal thruster form and so on for natural air-breathing will be interesting.

## 4.6 Conclusion of Multi-Pulse conditions

Repetitive pulse operation with a forced breath system is tested simulating gas intake during the rocket mode or the ramjet mode of the Microwave Rocket flights.

Impulse recovery at the second pulse count and maintenance of the steady impulse in the following pulses were achieved using the forced breath system. Moreover, the impulse dependences on the flow velocity of fresh air in a thruster, pulse repetition frequency, and thruster length were investigated. As a result, these dependences were expressed simply as a function of the partial filling rate which is a ratio of the volume replaced by fresh air during the pulse interval to the thruster volume in the case of Partial Filling Rate  $u/Lf > \text{Normalized Plasma Length } l$ . And, when the condition is Partial Filling Rate  $u/Lf < \text{Normalized Plasma Length } l$ , these dependences were expressed as a function of normalized plasma length  $l$  instead of thruster length  $L$ . The dependence showed that the impulse is fully recovered when the partial filling rate is greater than unity.

The thrust impulse was computed using an analytical engine cycle model based on a Pulse Detonation Engine model. Constant pressure heating in the plasma region was assumed instead of detonation heating. The results show a qualitative and quantitative agreement with the measured results. Using this model, the thrust impulse is predictable even in the cases when the partial filling rate is less than unity.

As mentioned above, it became possible to optimize the thrust in microwave repetitive pulse condition. A thrust can be chosen according to a design demand such as to obtain the maximum thrust or most efficient thrust like the conditions of microwave single pulse. Optimization of a thrust can be achieved by these results.

# Chapter 5

## Thrust Optimization

The thrust performance on single pulse conditions in Chapter3 and the thrust performance on multi-pulse conditions in Chapter4 are described. In this chapter, it argues about thrust optimization and flight mode of a microwave rocket is discussed based on these results, and the design of a microwave rocket is proposed.

### 5.1 Thrust Optimization in single pulse condition

The influence of pulse width, thruster length, pressure in the thruster, microwave power and gas species are argued for thrust performance in single pulse conditions of microwave. Now, these results are reconfirmed.

#### 1. Dependency on Pulse Width and Thruster Length

There are conditions which obtain largest thrust by long pulse width and most efficient thrust by optimization pulse width.

#### 2. Dependency on Pressure and Microwave Power

Thrust performance is optimized when the value of pressure and microwave electric power is more than a certain value. When it isn't satisfied this condition, thrust performance decreases drastically. Furthermore, although shock wave propagation velocity increased with decrease in pressure, ionization front propagation velocity decreased with decrease in pressure like the shock wave in the C-J MSD region and ionization front propagation velocity doesn't change or have steady change on the MSC region.

#### 3. Thrust Performance by Gaseous Species

A thrust become large when molecular weight is large. And a specific impulse become large when molecular weight is small.

That is, the thrust value on the single pulse conditions is determined as

$$I_{single} = C_m \cdot S_0 \cdot A \cdot \tau = C_{m_{max}} f(L_{thruster}, \tau) \cdot g(P, S_0) \cdot h(m) \quad (5.1)$$

Here,  $f(x)$  is the function which uses thruster length and plasma length for a variable,  $g(x)$  is the function which uses pressure and microwave power density for a variable, and  $h(x)$  are functions which uses a variable gaseous molecular weight for a variable.

As mentioned above, it is found that

**- When a high thrust is needed,**

- . Extend pulse width with thruster length as much as possible.
- . Heighten pressure and pressure in the thruster as much as possible.
- . Use gaseous whose molecular weight is large.

**- When high efficiency is needed,**

- . Optimize pulse width. In the case of a C-J MSD region, it is about 0.6. Since any thruster length doesn't present any problems, pulse width can be chosen by the thrust which is needed to obtain.
- . Heighten pressure and pressure in the thruster as much as possible.
- . Use gaseous whose molecular weight is small.

Therefore, it is necessary to optimize the thrust on single pulse conditions first according to demand performance and available conditions, when a microwave rocket is designed.

## 5.2 Thrust Optimization in multi-pulse condition

It argued about the influence of air-breathing, specifically, partial filling rate (the flow velocity in a thruster, microwave repetitive frequency, and thruster length) and pulse width, as thrust performance on multi-pulse conditions.

### • Dependence of thrust performance on the Partial Filling Rate

- . Normalized thrust 1 without the depression of thrust performance is obtained by more than partial filling rate 1. In the case of less than partial filling rate 1, the thrust performance according to MSC cycle calculation can be obtained.
- . Even when a partial filling rate is not fully obtained, thrust performance can be optimized by optimizing plasma length.
- . Even when without forced air-breathing, decrease of thrust performance become limited by natural air-breathing.

As mentioned above, the thrust value of a microwave rocket is determined as

$$F = I \cdot f = I_{\sin gle} \cdot i(u / Lf) \cdot f \quad (5.2)$$

Now,  $L$  is  $L_{thruster}$  at the time of  $u/L_{thruster}f > l$  and  $L=L_{plasma}$  at the time of  $u/L_{thruster}f < l$ . And, when the influence of natural air-breathing is larger than that of forced air-breathing, it is needed to consider to the influence of natural air-breathing. Here,  $i(x)$  is a function which makes a partial filling rate a variable.

As mentioned above, the following designs can be considered.

### - When air-breathing is enough obtained

The thrust is increased by raising microwave repetitive frequency and extending thruster length.

### - When air-breathing is not obtained enough

It can be optimized as a system of a microwave rocket by optimizing plasma length.

Therefore, it is necessary to optimize the thrust on multi-pulse conditions according to demand performance and the available conditions at the time of the design of a microwave rocket.

## 5.3 Thrust Optimization

The thrust of a microwave rocket is expressed as

$$\begin{aligned} F &= I \cdot f \\ &= C_m \cdot S_0 \cdot A \cdot \tau \cdot i(u / Lf) \cdot f \\ &= C_{m\max} \cdot f(L_{thruster}, \tau) \cdot g(p, S_0) \cdot h(m) \cdot i(u / Lf) \cdot f \end{aligned} \quad (5.3)$$

from Chapter5.1 and Chapter5.2.

It turns out that the thrust of a microwave rocket is determined intricately relating with various conditions from Equation 5.3. For example, when the pulse width and the thruster length of microwave are extended, the thrust on single pulse conditions become increase, but required air-breathing (= the flow velocity in a thruster) increases. That is, when required air-breathing is not obtained, thrust performance falls, and a thrust value may be decreased less than when pulse width or thruster length isn't extended. And, when microwave power is high in order to make propagation structure of the ionization wave front into a C-J MSD region at high altitude, the propagation velocity of the ionization front become very fast. Thereby, it is necessary to shorten pulse width and to increase microwave repetitive frequency. The further air-breathing is required in order to correspond to this demand. Therefore, it is necessary to design the system of a Microwave Rocket from design demand and required conditions. It is thought that the demand of air-breathing is increased for thrust recovery when other conditions are optimized. In the following section, the flight mode of microwave rocket



from a viewpoint of thrust optimization is discussed.

## **5.4 Flight Mode**

The thrust performance of the microwave rocket is clarified in the foregoing paragraph. The flight mode of Microwave Rocket is argued based on it. There are the three modes, such as Pulse Jet Mode, Air-Breathing Mode and Rocket Mode as flight mode of a microwave rocket which are shown in Figure. 5.1. The conditions and the generated thrust at the each mode are mentioned.

### **1 . Pulse-Jet Mode**

This flight mode is for the conditions of the low-speed flights such as the time of a launch, just after a launch and so on. In this mode, natural air-breathing from the back by pressure oscillation is used. For this reason, a partial filling rate may not be obtained enough. It becomes the trade-off of to prevented thrust depression by forced air-breathing using the mechanism of a turbine pump and so on or to obtain thrust which decreased to instead of the demerit of forced air-breathing system.

On the other hand, since air density is high just after a launch, air can be used. And since atmosphere pressure is still higher, a high thrust is expected compared with the condition of high altitude.

### **2 . Air-Breathing Mode**

This flight mode is for the high-speed flight of Microwave Rocket. In this mode, forced air-breathing is done by front air intake and thrust performance is secured. Therefore, air can be used as fuel. And, high pressure is maintainable in a thruster with ram compression. Therefore, the high thrust obtained by the high partial filling rate and high-pressure in a thruster is expected.

### **3 . Rocket Mode**

When a microwave rocket reaches high altitude, air density and atmosphere pressure become small, and it becomes impossible to obtain sufficient thrust performance. In

order to solve this problem, air-breathing is by the fuel carried in the microwave rocket at this flight mode. Although a partial filling rate become small, it is possible to optimize thrust performance by optimizing plasma length. And, air resistance decreases at this altitude, and thrust efficient becomes more important than thrust value. Therefore, it is needed to choose gaseous whose molecular weight is small since this mode require carrying fuel in flight. But since fuel tank becomes large when gaseous whose molecular weight is small, it becomes the trade-off of available thrust and the weight of a fuel tank.

The feature in each flight mode is summarized to below.

**Table 5.1 The feature in each flight mode**

Flight Mode	Flying Speed	Flight Level	Necessity for Fuel Loading
Pulse-Jet	Low	Near the ground	Unnecessary (Air)
Air-Breathing	High	-20km	Unnecessary (Air)
Rocket	-	20km-	Required

Partial Filling Rate	System Simplicity	Thrust	Thrust Efficiency
Low	Simple	Middle	Small-Middle
High	Slightly Complex	Large	High
Low	Slightly Simple	Small	Middle-High

The argument to the above is the flight mode which can be assume in Microwave Rocket and the thrust optimization of Microwave Rocket.

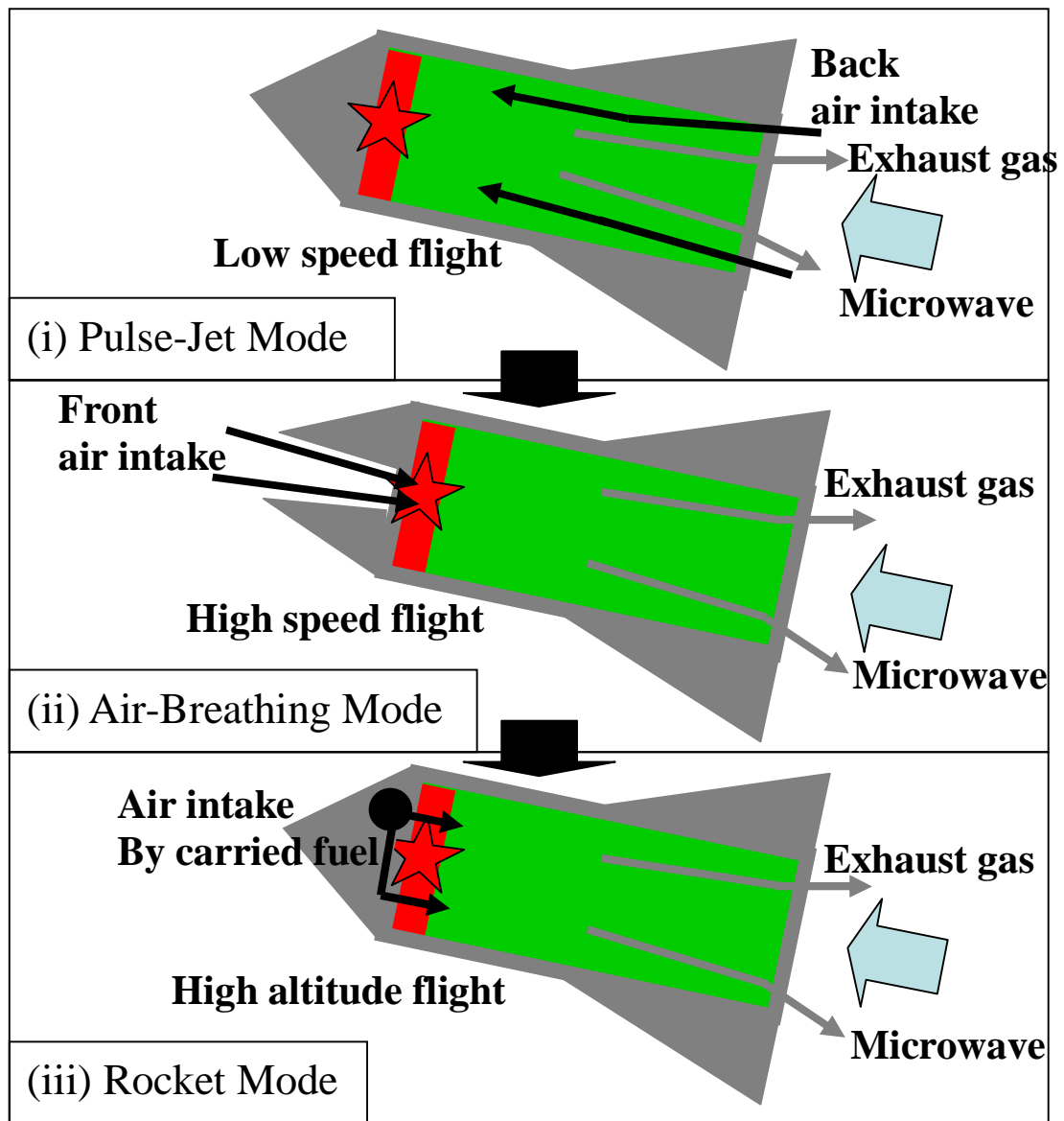


**FIGURE5.1.** Flight Mode of Microwave Rocket

## 5.4 Flight Analysis

Lastly, In order to verify the realization possibility of a microwave rocket, easy flight analysis was conducted. Weight 200[kg], a diameter 1[m], drag coefficient 0.3 is assumed, since it is expected that the demand of small satellite will increase in future. It is assumed that the output range of a gyrotron is variable about 1-20 [GW], and propagation structure of the

ionization front is C-J MSD region. The influence of diffusion and loss of microwave is ignored. As an environmental condition, it is set that gravity is constant at  $9.8 \text{ [m/s]}$ , and the air density near the ground is  $1.293 \text{ [kg/m}^3\text{]}$ , atmospheric pressure was derived from the approximation, and it was assumed that a pressure in the thruster was the same as atmosphere pressure. And, flying speed increases immediately from acceleration being very large and it is assumed that air-breathing in a thruster can be done enough.

The flying speed and the flight level by vertical launch when microwave power set to  $1.2 \text{ [GW]}$  are shown in Figures. 5.2 and 5.3. When a flight level goes up, air density is decreased and air resistance is decreased. But atmosphere pressure is decreased and the influences of thrust depression become large. For this reason, flying speed becomes steady around  $400 \text{ [m/s]}$ . In addition, the acceleration just after a launch is  $110 \text{ [m/s}^2\text{]}$ , and it cause concern about influence of the loading things according to raising microwave Power more.

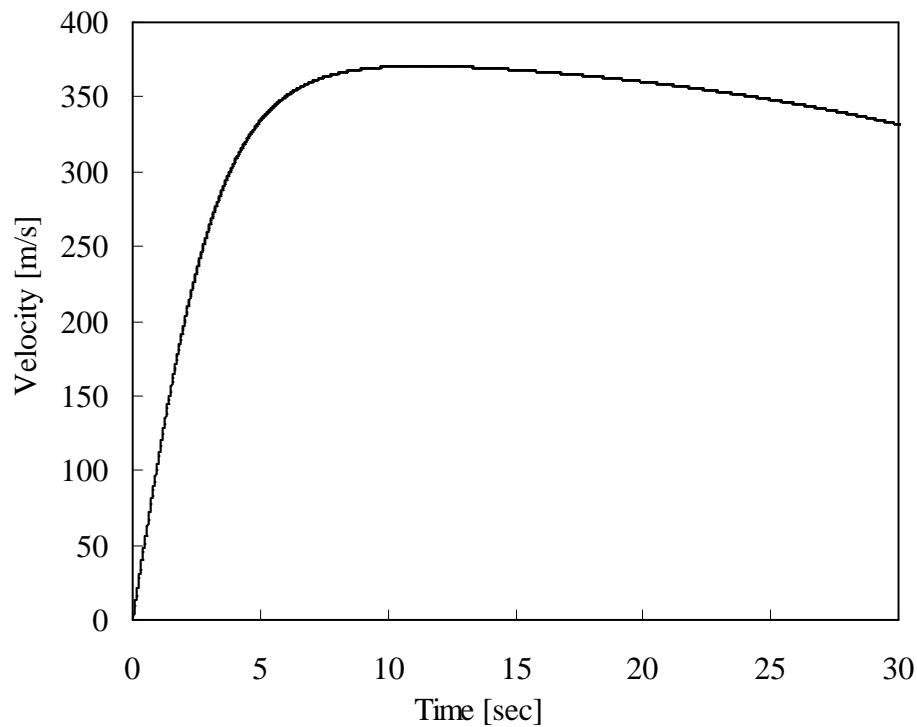


**FIGURE5.2.** Flying speed in flight analysis  
(vertical launch, microwave power:  $1.2 \text{ [GW]}$ )

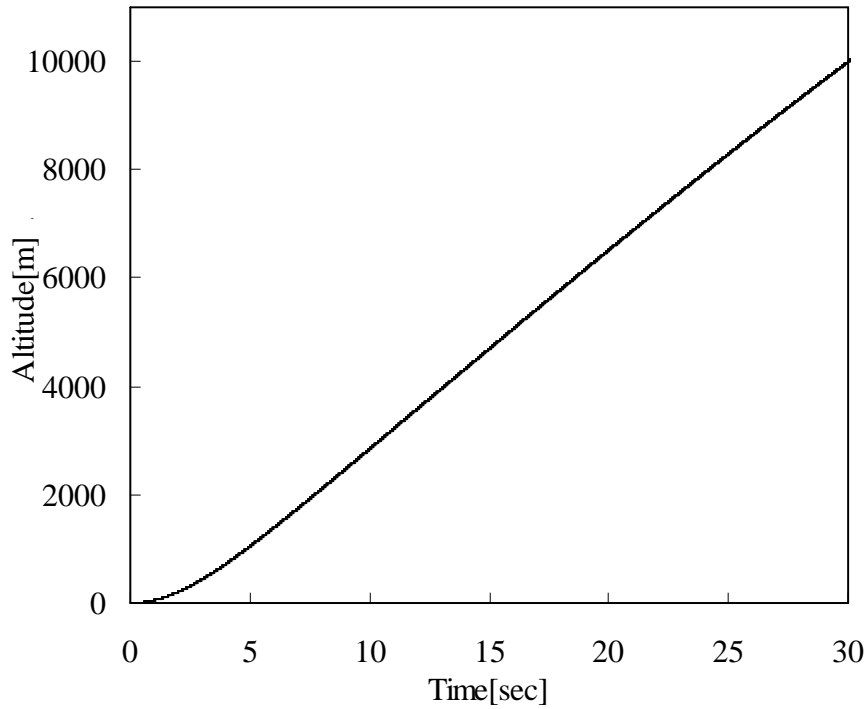


**FIGURE5.3.** Flying altitude in flight analysis  
(vertical launch, microwave power: 1.2 [GW])

Since it was thought that the influence of the thrust depression by decrease of atmosphere pressure is large, flight analysis was conducted assuming the parallel flight near ground where atmosphere pressure is high. The flying speed and the flight level by parallel flight when setting microwave power to 1.2 [GW] are shown in Figures. 5.4 and 5.5.

In this case, atmosphere pressure is maintained constant and reduction of the thrust under this influence is not produced. But air resistance increase according to the increment in speed, and termination speed become around 400 [m/s]. And, the termination speed is almost same compared with the top speed in the case of a vertical flight. Thus, it turns out that the system of going up after earning speed by parallel flight is not effective as Microwave Rocket.

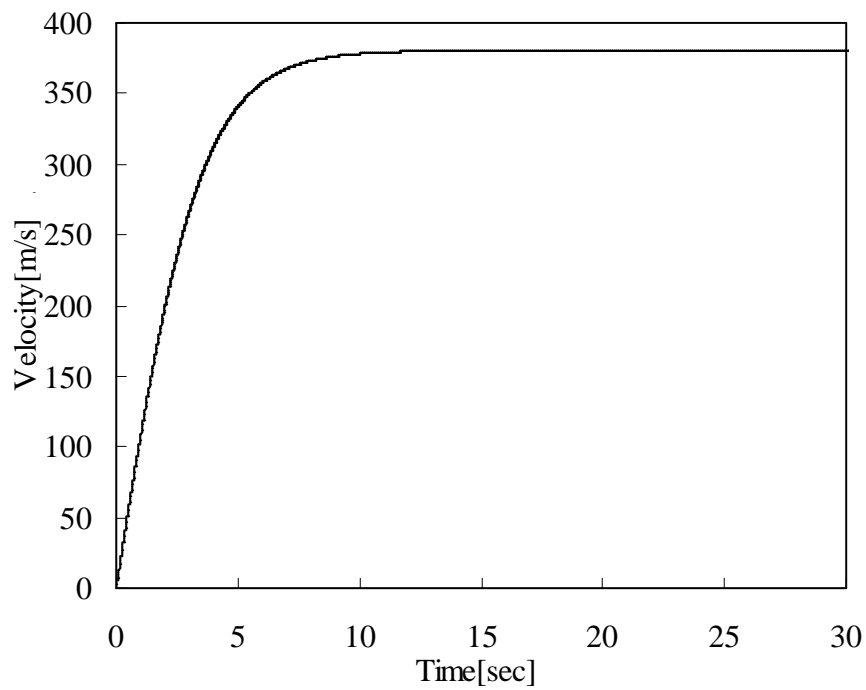


**FIGURE5.4.** Flying speed in flight analysis  
(parallel flight, microwave electric power Power:1.2 [GW])

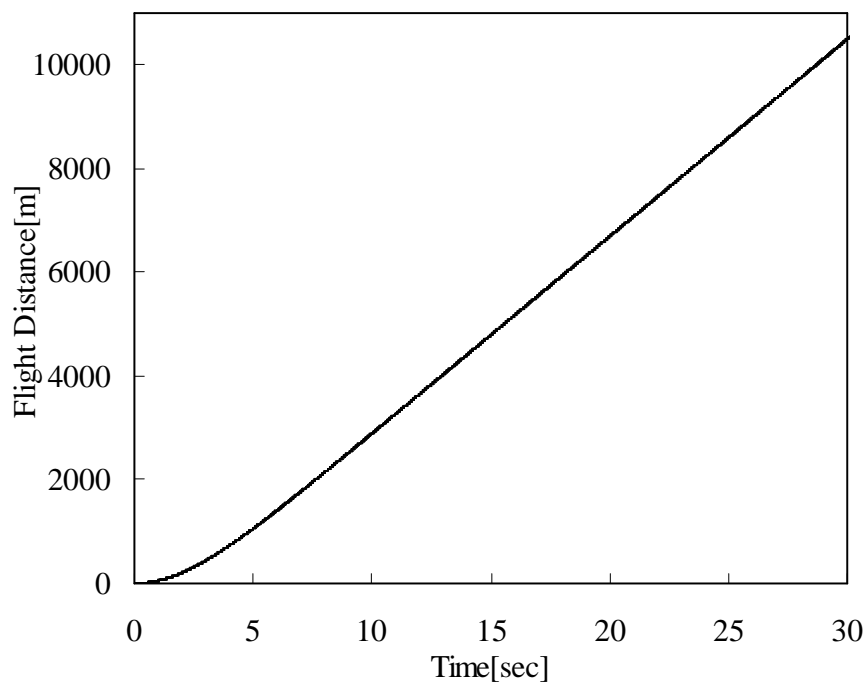


**FIGURE5.5.** Flight distance in flight analysis  
(parallel launch, microwave Power:1.2 [GW])

The problem is thrust depression by reduction of atmospheric pressure and thrust not increasing by air resistance. Therefore, the solution is to obtain air resistance reduction by vertical flight and stopping the thrust reduction by atmosphere pressure reduction. The flying speed and the flight level by vertical flight when the thrust value is assumed to be steady are shown in Figures 5.6 and 5.7.

As shown in Fig. 5.6, flying speed is increased favorably under thrust steady assumption. Now, let us consider how thrust constancy is obtained. The method of compensating reduction in a thrust by the increment in microwave Power is proposed. For example, when a thrust becomes half by reduction of atmosphere pressure, a thrust is kept constant by doubling microwave power to supply. The normalized microwave power by the microwave power just after launch is shown in Figure 5.8 and the integrated normalized microwave power is shown in Figure 5.9.

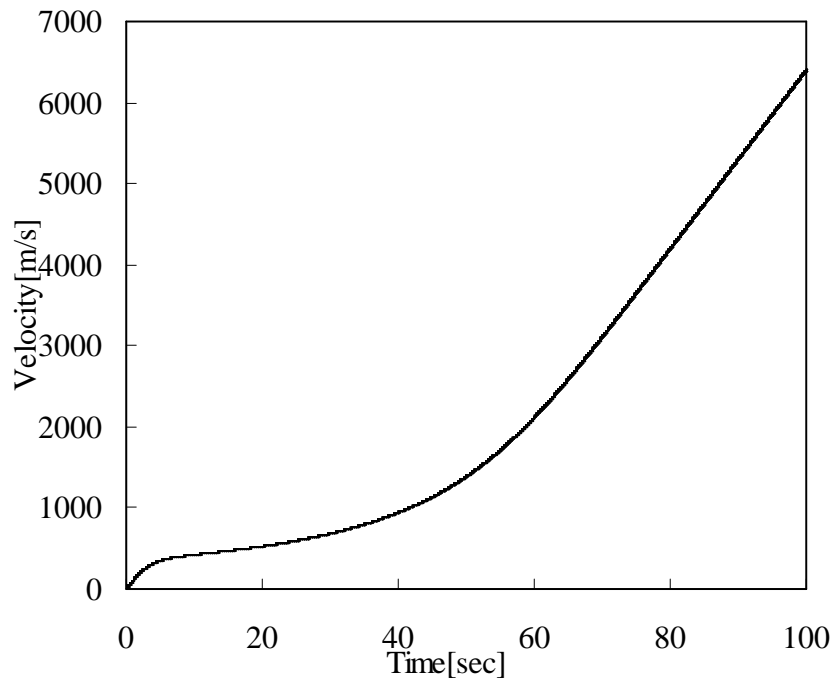


**FIGURE 5.6.** Flying speed in flight analysis (vertical launch, thrust is constant)

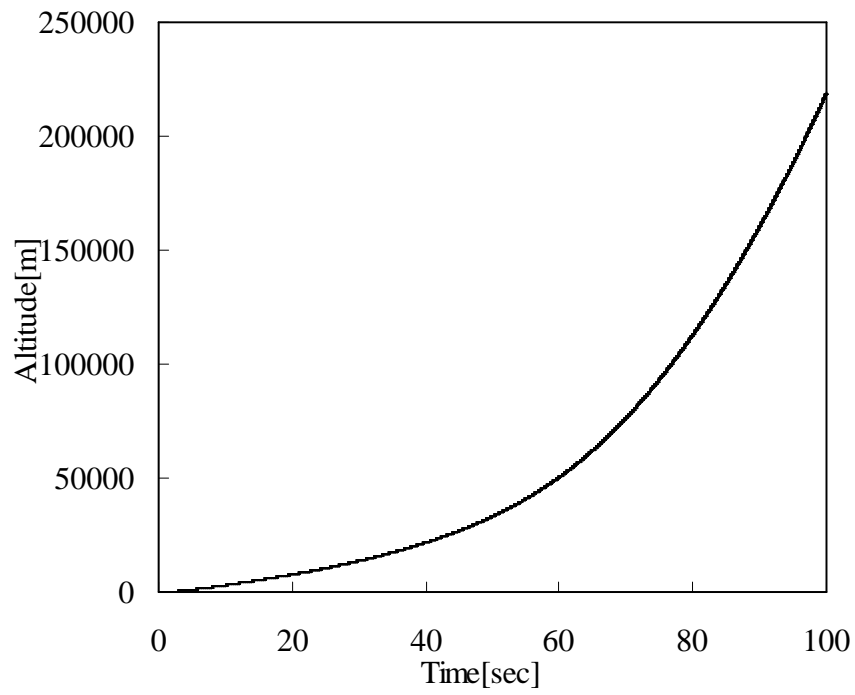


**FIGURE5.7.** The fight level in flight analysis (vertical launch, thrust is constant)

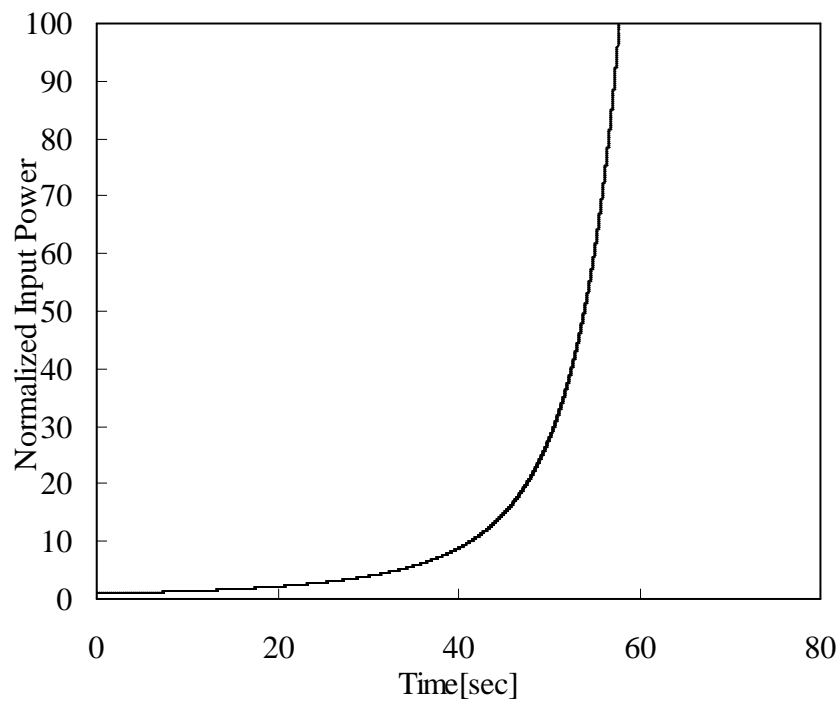


**FIGURE5.8.** Normalized microwave power



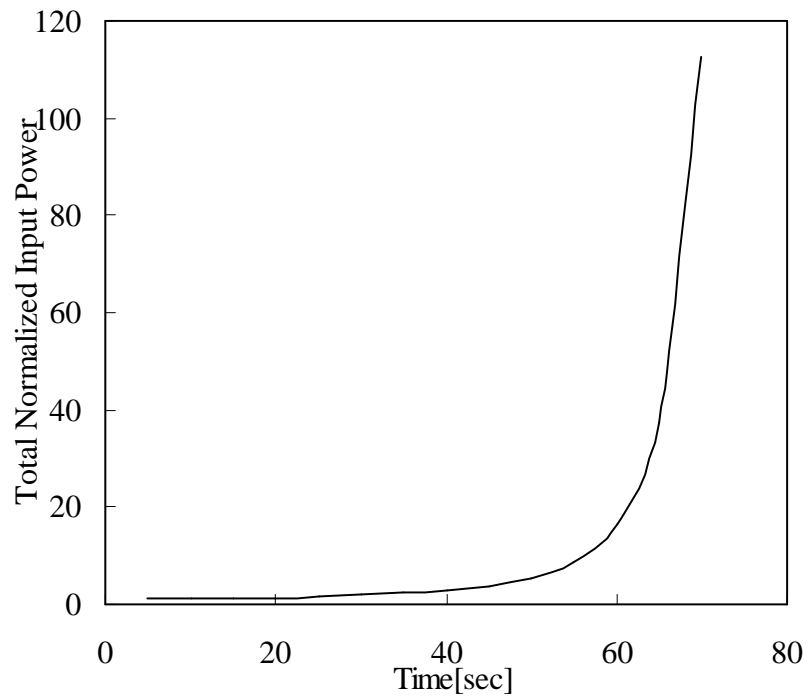


**FIGURE5.9.** Integrated normalized microwave power

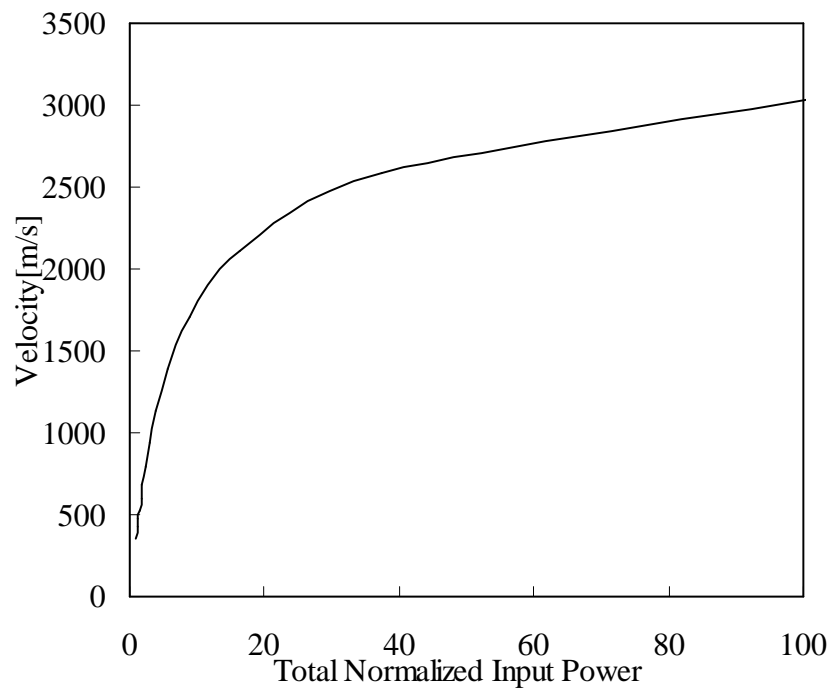


**FIGURE5.10.** Flying speed dependence on integrated normalized microwave power

Fig. 5.8 shows that microwave power is increasing rapidly in around 40 second after-launch and altitude of 4km. Fig. 5.9 shows that the integrated value also increases rapidly in about 60 seconds. Let us consider appropriate point to increase the microwave power. The flying speed dependence on the integrated normalized microwave power is shown in Fig. 5.10. Although the flying speed is increased drastically until integrated normalized microwave power is around 20, the rise of flying speed is limited more than 20. It is found that the flight time is about 60 seconds from Fig. 5.9, and more than 200 [m/s] of the flight speed is obtained from Fig. 5.6. That is, the 6 times flying speed can be obtained by increasing 20 times integrated microwave power to supply in the thruster without changing the design of microwave. This means that flying speed can be optimized by optimizing microwave power. And, it is shown that the relation of microwave power and obtained flying speed become one of the important in the case of the microwave rocket design. It is possible to suggest the timing of a mode change from Air-Breathing Mode to Rocket Mode by using these results.

And, it is expected that the high pressure more than atmosphere pressure is maintained by ram compression in a thruster in Air-Breathing Mode, and the higher flying speed is expected in an actual flight.

# Chapter 6

## Conclusion

In this research, the thrust under various conditions is verified. Flight mode, flying speed and so on were analyzed above, thrust optimization of the microwave rocket was done and the implement ability of a microwave rocket is argued.

### 1. Thrust Optimization

A thrust is determined by thruster length, microwave pulse width, pressure, microwave power density, gaseous species, partial filling rate and so on, and is expressed by

$$\begin{aligned} F &= I \cdot f \\ &= C_m \cdot S_0 \cdot A \cdot \tau \cdot i(u / Lf) \cdot f \\ &= C_{m \max} \cdot f(L_{thruster}, \tau) \cdot g(p, S_0) \cdot h(m) \cdot i(u / Lf) \cdot f \end{aligned} \quad (5.3)$$

The thrust can be optimized for the demanded performance.

Verification of the influence for the thrust performance by the difference of gas species, and verification of the thrust performance in Overdriven MSD region are interesting.

### 2. Flight Mode

In order to solve thrust depression, forced air-breathing system is needed for to exhaust the remained hot gas in a thruster and to inhale fresh air in a thruster. The following three flight modes can be considered in the flight mode of a microwave rocket.

#### . Pulse-Jet Mode

Back air intake is done in the condition of a low-speed flight. This flight mode is effective just after launch. Verification of thruster form for efficient natural air-breathing and the maximum of microwave repetitive frequency are interesting in future.

#### . Air-Breathing Mode

Front air intake is done in the condition of a high-speed flight. Very high thrust can be obtained, since enough flying speed and high air density can be available. Therefore, it is found that this mode is quite effective. Verification of "the influence of temperature" and "the influence on the ionization wave and the shock wave propagation propagated in a thruster" will be interesting for ram compression.

#### . Rocket Mode

Intake from the carrying fuel in the thruster is done in a high-altitude flight. At high altitude, this flight mode is effective, and high thrust performance can be maintained by optimizing microwave conditions. And, the microwave rocket can use any gaseous as fuel unlike other chemistry organizations. Therefore, degree of freedom of a design is quite high.

### **3. Flight Analysis**

The flight speed of microwave rocket dependence on microwave power becomes a very important index in designing microwave rocket. It is because microwave power to supply and a flight mode change is determined by this.

It is possible to reach to the 1st cosmic velocity by only changing microwave electric power if the enough output of a gyrotron to be obtained, even if pessimistic calculation is done. This means that the realization possibility of a microwave rocket increases very much. Furthermore, the realization possible is high by less electric power by the high-pressure maintenance in the thruster by ram compression and establishment of forced air-breathing system.

In any case, it is indispensable that the gyrotron which is a source of a microwave oscillation is developed, and a very high beam output is obtained by phased array technology for microwave rocket realization. Therefore, the more technical development of a gyrotron is strongly expected.

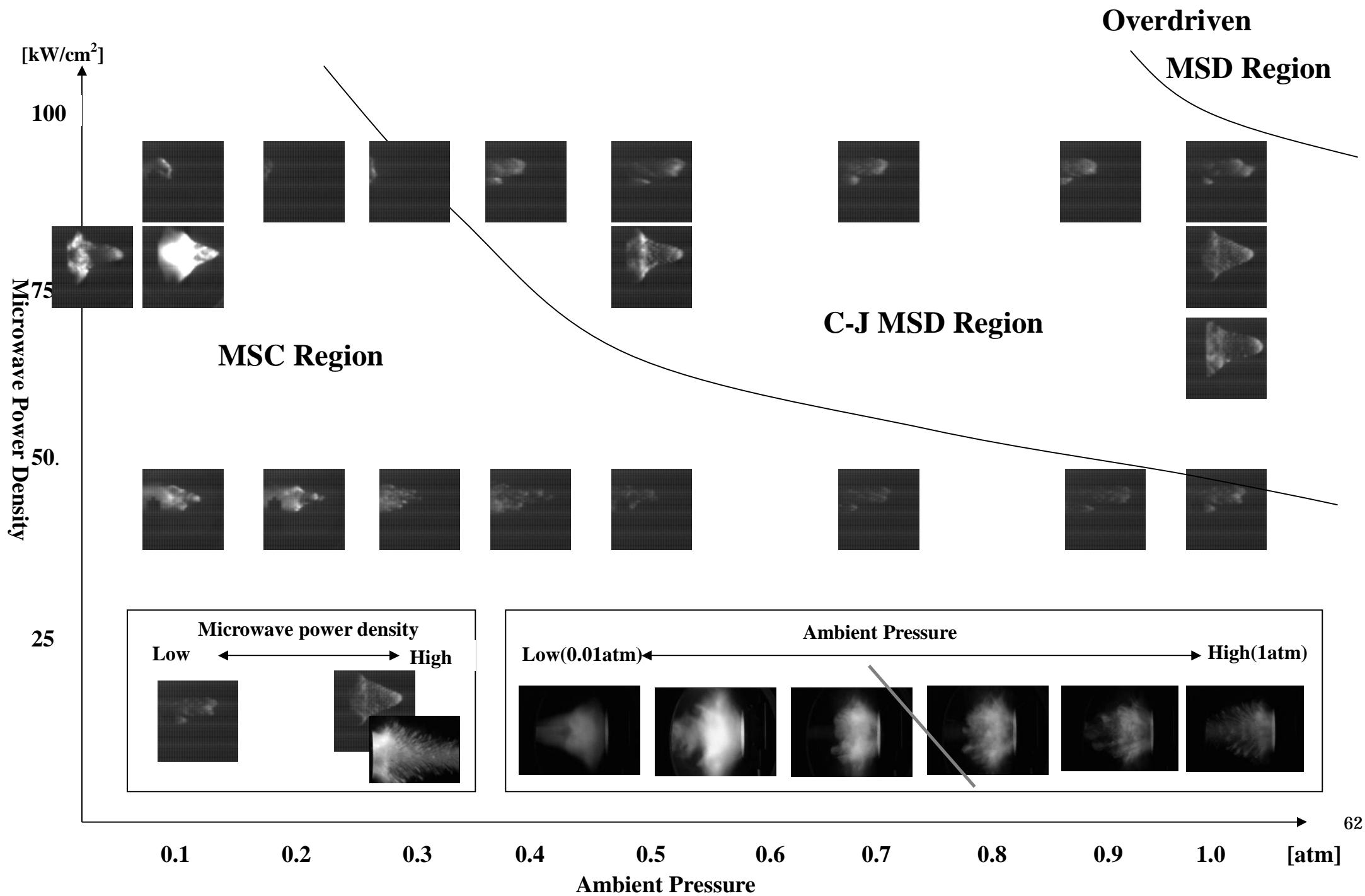
## References

1. 牛尾正人, "宇宙吸込式レーザー推進に要するレーザーパワーの研究", Master Thesis of The Universit of Tokyo 2003
2. Brikan M.A., "Laser Propulsion: Research Status and Needs", Journal of Propulsion and Power, 8, (1992), pp. 354-360
3. Kantrowitz A., "Propulsion to Orbit by Ground-Based Lasers", Astronautics and Aeronautics, pp. 74-76, 1972
4. Raizer Y.P., "Laser-Induced Discharge Phenomena", Consultants Bureau, New York and London, 1977, Ch.6
5. Myrabo L.N., Messitt D.G. and Mead F.G.Jr, "Ground and Flight Test of a Laser Propelled Vehicle", AIAA Paper 98-1001, 1998
6. Myrabo L.N., "World Record Flights of Beam-Riding Rocket Lightcraft - Demonstration of "Disruptive" Propulsion Technology", AIAA Paper 01-3798, 2001
7. K. Sakamoto, A. Kasugai, K. Takahashi, R. Minami, N. Kobayashi, and K. Kajiwara, Nature Pysics, 3(6):411-414, 2007
8. A. Kasugai, K. Sakamoto, R. Minami, K. Takahashi, and T. Imai, "Study of millimeter wave high-power gyrotron for long pulse operation", Nuclear Instrument and Method in Physics Research A, 528:110-114, 2004
9. K. Sakamoto, "Application of plasma heating technology for frontier science", Proceedings of Plasma Science Symposium 2005 and The 22nd symposium on Plasma Proceeding, 2005
10. Nakagawa T., Mihara Y., Komurasaki K., Takahashi K., Sakamoto K., and Imai T., "Propulsive Impulse Measurement of a Microwave-Boosted Vehicle in the Atmosphere", Journal of Spacecraft and Rockets, Vol. 41, 2004, pp. 151-153
11. Katsurayama H., Komurasaki K., and Arakawa Y., "Feasibility for the Orbital Launch by Pulse Laser Propulsion", Journal of Space Technology and Science, Vol. 20, No. 2, 2005, pp. 32-42
12. Oda Y., Ushio M., Komurasaki K., Takahashi K., Kasugai A., and Sakamoto K., "A Multi Pulsed Flight Experiment of a Microwave Beaming Thruster", 3rd International Symposium on Beamed Energy Propulsion, Troy, NY, 2004, pp. 295-302
13. Oda Y., Ushio M., Komurasaki K., Takahashi K., Kasugai A., and Sakamoto K., "Pressure History Measurement in a Microwave Beaming Thruster", 4th International Symposium on Beamed Energy Propulsion, Nara, Japan, 2005
14. Oda Y., Komurasaki K., Takahashi K., Kasugai A., and Sakamoto K., "Experimental study on microwave beaming propulsion using a 1MW-class gyrotron", 56th International Astronautical Congress, Fukuoka, Japan, 2005
15. Oda Y., Kawamura K., Komurasaki K., Takahashi K., Kasugai A., and Sakamoto K., "An Experimental Study on a Thrust Generation Model for Microwave Beamed Energy Propulsion", AIAA 2006-0765

16. Oda Y., Shibata T., Komurasaki K., Takahashi K., Kasugai A., and Sakamoto K., "A Plasma and Shockwave Observation with Pulse Repetition in a Microwave Boosted Thruster", AIAA 2006-4631
17. Oda Y., Shibata T., Komurasaki K., Takahashi K., Kasugai A., and Sakamoto K., "An Experimental Observation for the Shock Wave Driven by Atmospheric Microwave Plasma in a Microwave Rocket", AIAA 2007-4592
18. Oda Y., Shibata T., Komurasaki K., Takahashi K., Kasugai A., and Sakamoto K., "A thrust generation model of microwave rocket", Journal of Space Technology and Science (in print)
19. Bussing T., and Pappas G., "An Introduction to Pulse Detonation Engines", AIAA 94-0263 (1994)
20. Endo T., Kasahara J., Matsuo A., Inaba K., Sato S., and Fujiwara T., "Pressure History at the Thrust Wall of Simplified Pulse Detonation Engine", AIAA Journal, Vol. 42, No. 9, 2004, pp. 1921-1930
21. Sakamoto, K., Kasugai, A., Takahashi, K., Minami, R., Kobayashi, N., and Kajiura, K., "Achievement of robust high-efficiency 1MW oscillation in the hard-self-excitation region by a 170GHz continuous-wave gyrotron", Nature Physics, Vol. 3, No. 6, 2007, pp.411-414
22. T. Shibata et al., Proceeding of 5th International Symposium on Beamed Energy Propulsion (2007) in print.
23. 嶋田豊, 柴田鉄平, 小田靖久, 小紫公也, 荒川義博, "マイクロ波ロケットの推力発生家庭に関する数値解析", 第 22 回数値流体力学シンポジウム
24. 堤井信力, "プラズマ基礎工学", 内田老鶴圃, 1986
25. Yasuhisa Oda, Kimiya Komurasaki, Koji Takahashi, Atsushi Kasugai, Keishi Sakamoto, "Plasma generation using high-power millimeter wave beam and its application for thrust generation", Journal of Applied Physics, Vol.100, 2006, 113308 (4pages)
26. 柴田鉄平, 小田靖久, 小紫公也, 高橋幸司, 春日井敦, 坂本慶司, "マイクロ波ロケットの推力発生モデルへの給排気過程の影響", 平成 19 年度宇宙輸送シンポジウム
27. 小田靖久, 柴田鉄平, 小紫公也, 高橋幸司, 春日井敦, 坂本慶司, "PDE 型マイクロ波ロケット内における爆轟波形成", 平成 18 年度宇宙輸送シンポジウム
28. 松尾 一泰, "圧縮性流体力学 内部流れの理論と解析", 理工学社, 1994

# Appendix

- Graph of photograph ionization front propagation by High speed of plasma  
(  $x$  axis : Pressure,  $y$  axis : microwave power density )





## 修士論文に関する発表一覧

1. Yuya Shiraishi, Yasuhisa Oda, Teppei Shibata, Kimiya Komurasaki, Koji Takahashi, Atsushi Kasugai and Keishi Sakamoto, "Air Breathing Processes in a Repetitively Pulsed Microwave Rocket", 46th AIAA Aerospace Sciences Meeting, January 7-10, 2008, Reno
2. Yuya Shiraishi, "Thrust Measurement of Microwave Rocket with Repetitive Pulse Operation", 26th International Symposium on Space Technology and Science, June 1-8, 2008, Hamamatsu
3. 白石 裕也, 山口 敏和, 小紫 公也, 小田靖久, 梶原健, 高橋幸司, 春日井敦, 坂本慶司, "前方吸気を想定したマイクロ波ロケットの部分充填率による推力最適化", 平成 20 年度宇宙輸送シンポジウム, January 19-20, 2009, 相模原
4. 白石 裕也, 山口 敏和, 小紫 公也, 小田靖久, 梶原健, 高橋幸司, 春日井敦, 坂本慶司, " マイクロ波電力および雰囲気圧力によるマイクロ波ロケットの推力最適化", 第 49 回 航空原動機・宇宙推進講演会, March 5-6, 2009, 長崎